Journal of Medicinal Chemistry

Article

pubs.acs.org/jmc

Discovery of Small Molecules for Up-Regulating the Translation of Antiamyloidogenic Secretase, a Disintegrin and Metalloproteinase 10 (ADAM10), by Binding to the G-Quadruplex-Forming Sequence in the 5′ Untranslated Region (UTR) of Its mRNA

Jie Dai,‡ Zhen-Quan Liu,‡ Xiao-Qin Wang, Jing Lin, Pei-Fen Yao, Shi-Liang Huang, Tian-Miao Ou, Jia-Heng Tan, Ding Li, Lian-Quan Gu, and Zhi-Shu Huang*

School of Pharmaceutical Sciences, Sun Yat-sen University, Guangzhou 510006, People's Republic of China

Supporting Information

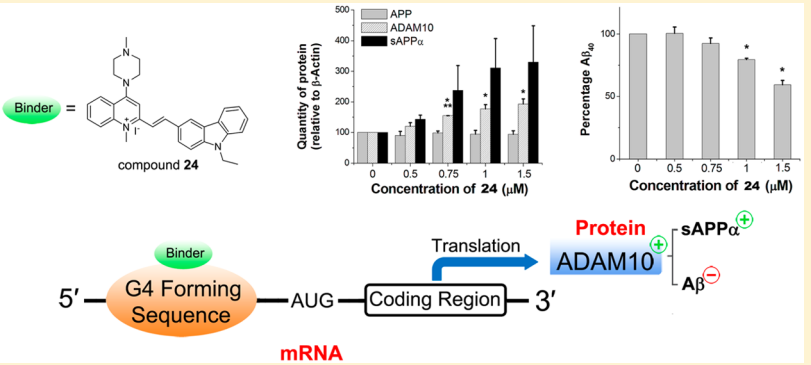

ABSTRACT: Up-regulation of a disintegrin and metalloproteinase 10 (ADAM10) to prevent the formation of β-amyloid (Aβ) peptides might be a promising strategy to treat Alzheimer's disease (AD). RNA G-quadruplex motif within the 5′-UTR of the ADAM10 mRNA is an inhibitory element for ADAM10 translation. Thus, mitigation of the suppressive effect of this motif using an RNA G-quadruplex-forming G-rich sequence (QGRS) binder might be a new approach for AD therapy. Herein, a series of new methylquinolinium derivatives were synthesized and screened by surface plasmon resonance (SPR) and the dual-luciferase reporter assay. Among them, compound **24** showed selective affinity for the QGRS of ADAM10 and could strongly up-regulate the translation of it. Moreover, treatment with **24** led to a significant increase of the secretion of sAPPα, consequently decreasing the Aβ_{40} in cellular. These results illustrate that the interaction between the RNA QGRS and a small molecule may be a new molecular strategy to modulate the translation of ADAM10.

INTRODUCTION

Alzheimer's disease (AD) is a common neurodegenerative disorder involving a progressive loss of cognitive functions. β-Amyloid (Aβ) peptide is believed to play a significant role in the neurotoxicity and the development of AD.[1] Neurotoxic Aβ results from the amyloidogenic processing of the amyloid precursor protein (APP) in which it is sequentially cleaved by β- and γ-secretase.[1,2] Alternatively, a third protease, α-secretase, can cleave APP within its amyloid domain and liberate a secreted product, sAPPα, that has neuroprotective properties,[3,4] thereby preventing the production of the neurotoxic Aβ (Figure 1). Moreover, it is well established that the regulated component of α-secretase can compete with β-secretase and thereby reduce the generation of neurotoxic Aβ, suggesting that a pharmacological activation of α-secretase could improve the therapeutic approach in AD.[5] Some members of a large family of disintegrin and metalloproteinases (ADAM) have been shown to exert α-secretase activity.[6−9] Among these, ADAM10 has been identified the major member for the α-secretase.[10−16] Clinical studies have provided evidence that ADAM10 is a candidate AD susceptibility gene,[11] and significantly reduced levels of both ADAM10 and sAPPα are present in the platelets of AD patients.[13] Therefore, up-regulation of ADAM10 and/or stimulation of ADAM10 activity with the consequence of reducing the generation of Aβ might be a promising strategy to treat AD.

The strategies for the modulation of ADAM10 cleavage can be broadly classified into four groups: the transcriptional level, translational level, enzymatic activity, and indirect modulation (Figure 1). Progress toward development of a direct activator of α-secretase as a drug treatment for AD has not been encouraging.[17] Transcriptional modulators including acitretin,[14] a vitamin A derivative, as well as GABA-A receptor modulators including etazolate hydrochloride (EHT-0202)[18,19] can promote sAPPα secretion and are considered to be promising drug

Received: January 26, 2015

DOI: 10.1021/acs.jmedchem.5b00139
J. Med. Chem. XXXX, XXX, XXX−XXX

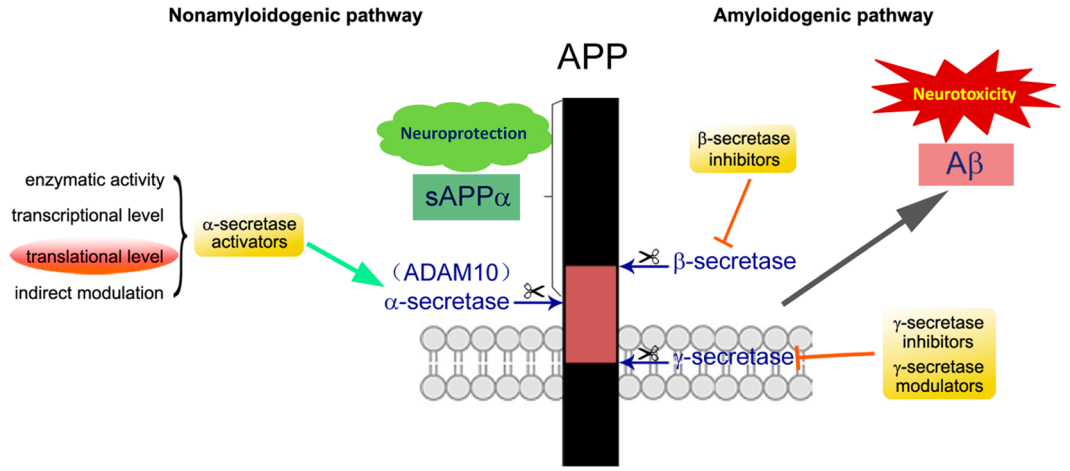

Figure 1. Schematic representation of the APP processing pathway and strategy to use small molecules to reduce Aβ. APP ectodomain shedding is mediated by either an α-secretase or the β-secretase. While the APP ectodomain released by α-secretase liberates the neuroprotective sAPPα, β-secretase/γ-secretase cleavage leads to the release of neurotoxic Aβ peptides. The methods targeting Aβ can be classified into three groups: the enhancement of α-secretase activity and the inhibition of β-secretase or γ-secretase cleavage. Among these, regulation of the translational level of α-secretase (ADAM10) has stimulated the most interest.

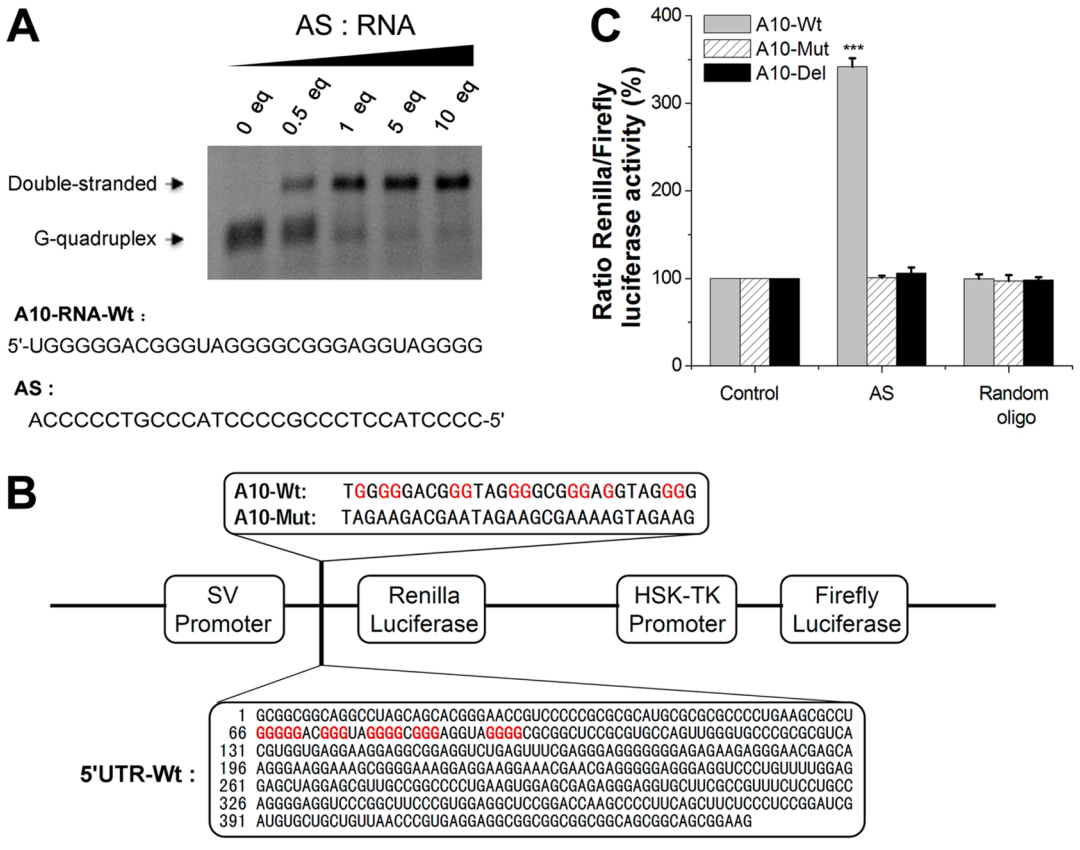

Figure 2. Antisense oligonucleotide AS destabilizes the G-quadruplexes of the ADAM10 mRNA to enhance luciferase expression. (A) AS traps RNA G-quadruplex motifs into double-stranded structures in a concentration-dependent manner. A fluorescently labeled A10-RNA-Wt sequence (Cy3 and Cy5 at its 3′ and 5′ ends, respectively) was titrated with increasing concentrations of the AS deoxyoligonucleotide and analyzed using a native gel electrophoresis assay. (B) Schematic representation of the plasmids used for the dual-luciferase reporter gene assays. The wild-type QGRS (A10-Wt) of the ADAM10 5′-UTR or its mutated variants (A10-Mut) and the wild-type full-length 5′-UTR of ADAM10 (5′UTR-Wt) or its QGRS motif-mutated variants (5′UTR-Mut) were cloned directly in front of the *Renilla* coding region.[22] (C) Effect of antisense deoxyoligonucleotides on the dual-luciferase assays. The dual-luciferase assay was performed at 24 h post-transfection with AS or random deoxyoligonucleotides. The fold changes in expression were calculated relative to blank control (control was set as 1). All data are expressed as the mean ± SD from three independent experiments. The symbols *** indicate significant differences at $P < 0.001$ vs control.

candidates for AD.[17,20] However, attenuation of AD symptoms by these drugs has not been demonstrated in patients.[17] Recently, there has been increased interest in the regulation of ADAM10 expression through mechanisms involving the 5′

DOI: 10.1021/acs.jmedchem.5b00139
J. Med. Chem. XXXX, XXX, XXX−XXX

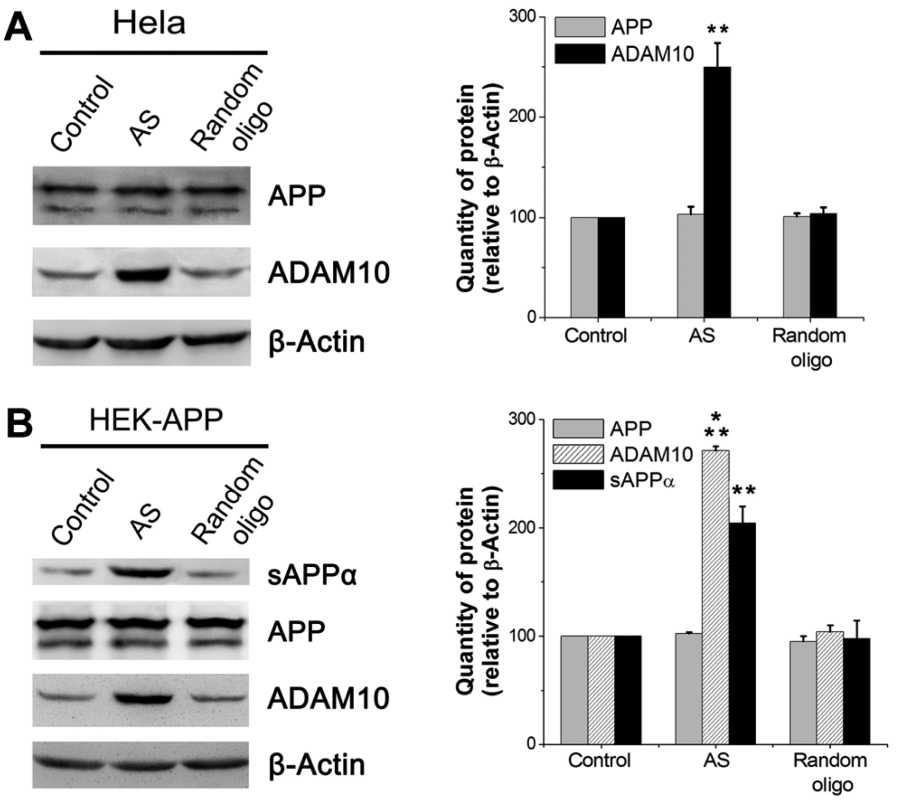

Figure 3. Effect of the antisense oligonucleotide AS on ADAM10 translation. (A) Western blot showing the levels of APP, ADAM10, and β-actin proteins in HeLa cells transfected with 200 nM AS or random deoxyoligonucleotides. (B) Western blot showing the levels of sAPPα, APP, ADAM10, and β-actin proteins in HEK-APP cells transfected with 200 nM AS or random deoxyoligonucleotides. All data were normalized to β-actin, and the fold changes in expression were calculated relative to the blank control (the control was set to 1). All data are expressed as the mean ± SD from three independent experiments. The symbols ** and *** indicate significant differences at $P < 0.01$ and $P < 0.001$ vs control.

untranslated region (UTR) of the ADAM10 mRNA.[21] Importantly, translation of ADAM10 is suppressed by its long GC-rich 5′-UTR, which contains a G-rich sequence that can form stable RNA G-quadruplex secondary structures.[22] Further study has demonstrated that the presence of this RNA G-rich sequence in an overexpression construct of ADAM10 caused a reduction in the protein levels, while the mRNA levels were not altered. Mutation of the G-quadruplex motif results in increased ADAM10 translation and consistently promoted the secretion of sAPPα.[22] These data provide an alternative basis to hypothesize that the RNA G-quadruplex-forming G-rich sequence (QGRS) is a new molecular target for therapeutic efforts to up-regulate ADAM10 expression.[23]

An increasing number of reports in the past few years have focused on the RNA G-quadruplex within the 5′-UTR because of its critical biological functions especially in translation.[24] Down-regulation of translation by RNA G-quadruplex regions has been reported for several genes including *EBNA1*,[25] *N-ras*,[26] *Zic-1*,[27] *Bcl-2*,[28] and others,[29] and up-regulation of translation by this structure has also been reported for *VEGF*.[30] More significantly, regulation of translation by exogenous factors, such as small molecules and antisense oligonucleotides (ASO) that bind to the RNA G-quadruplex within the 5′-UTR of mRNAs, has been proven to be effective.[25,31,32] Several examples so far suggest a mechanism by which small molecules act as RNA G-quadruplex binders to inhibit translation via stabilization of the 5′-UTR RNA G-quadruplex structure.[33−37] For example, Pierre Murat et al. demonstrated that targeting the *EBNA1* mRNA with a small molecule that stabilized the G-quadruplex structures inhibits the translation of the *EBNA1* mRNA and decreases antigen presentation.[25] On the other hand, G-quadruplex binders have rarely been shown to increase the translation efficiency. The only example is the cationic porphyrin TMPyP4, which has been reported to destabilize the $(CGG)_n$ intramolecular quadruplex structure and increase translation efficiency of the 5′-UTR mRNA.[38] These combined data suggest a new strategy by which exogenous factors such as small molecules may modify the inhibitory effect of the G-quadruplexes on translation.

Here, we report the effect of exogenous factors on the elimination of the inhibitory effect of the G-quadruplexes located in the 5′-UTR of ADAM10 on the translation of the mRNA, as well as the discovery of translational up-regulators, the design, synthesis, and structure−activity relationships (SARs) of new methylquinolinium derivatives that target the QGRS in the 5′-UTR of the ADAM10 mRNA, and the in-depth evaluation of the optimized compound.

RESULTS AND DISCUSSION

DNA Antisense Oligonucleotides Targeting RNA QGRS Increase the Translation Efficiency of ADAM10. Mutation of the G-quadruplex motif in 5′-UTR resulted in increased ADAM10 translation and consistently promoted the secretion of sAPPα.[22] However, this study provided no evidence for the ability of exogenous factors to eliminate the inhibitory effect of the G-quadruplexes on the translation of the ADAM10 mRNA. Recently, oligonucleotides-based strategies

DOI: 10.1021/acs.jmedchem.5b00139
J. Med. Chem. XXXX, XXX, XXX−XXX

Table 1. Binding Data for the Interaction between RNA and Designed Analogs Using the SPR Assay

	Compound	R	SPR(K_D/μM)[a]
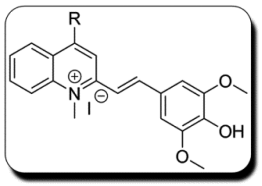	**1**	H	20.5
	2		27.1
	3		25.0
	4	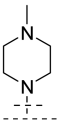	16.5
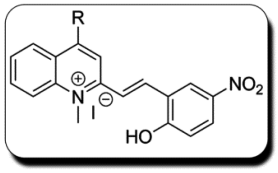	**5**	H	46.3
	6		>50
	7		>50
	8	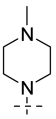	16.3

[a]K_D for different compounds toward the A10-RNA-Wt sequence as determined using SPR. Compounds that did not achieve saturation state at the highest tested concentration (50 μM) are noted. Compounds noted as >50 μM are considered to have low affinity for the RNA QGRS.

that, using antisense oligonucleotides to modulate RNA G-quadruplexes folding, affect the translation of specific mRNAs were on the rise.[25,32] Pierre Murat et al. were the first to demonstrate that destabilization of G-quadruplexes within the *EBNA1* mRNA using antisense oligonucleotides (both the RNA antisense oligonucleotide and its DNA analog) increases *EBNA1* mRNA translation.[25] According to this strategy, and with the goal of verifying the feasibility of designing small-molecule modulators of QGRS within ADAM10 mRNA to regulate ADAM10 translation, in an initial study we explored the effect of DNA antisense oligonucleotides on the elimination of inhibitory effect of G-quadruplexes in the 5′-UTR on ADAM10 mRNA translation. First, the results of native gel electrophoresis assays showed that titration with increasing concentrations of DNA antisense oligonucleotides (AS) caused the G-quadruplexes bands (lower bands) to gradually disappear, indicating the ability of the antisense oligonucleotides to trap the G-quadruplex motifs of ADAM10 into double-stranded structures (upper bands) (Figure 2A).

The effects of the AS deoxyoligonucleotide on translation were subsequently detected using the dual-luciferase reporter system, which is an appropriate system for evaluating the capacity of exogenous factors to regulate gene expression. For these experiments, the reporter plasmid described previously,[22] carrying the ADAM10 G-quadruplex motif (A10-Wt) in front of the *Renilla* luciferase in the psi-CHECK-2 vector (Figure 2B), was used. The G-quadruplex motif mutant variant (A10-Mut) and psi-CHECK-2 blank vector (A10-Del) were used as system controls,[22] and transfection with no oligonucleotide or a random deoxyoligonucleotide was used as negative control in this experiment. The data presented in Figure 2C demonstrate a 3.4-fold increase in the luciferase expression following treatment for 24 h with the AS deoxyoligonucleotide in the cells containing the A10-Wt plasmid. As expected, the effect of the AS deoxyoligonucleotide on luciferase expression in the cells containing the mutant or blank plasmids was insignificant. Furthermore, the deoxyoligonucleotide-free control group and random deoxyoligonucleotide group also demonstrated no obvious change in luciferase expression. Next, we asked whether the AS oligonucleotide was capable of improving the expression level of genomic ADAM10 in a cellular system. To address this question, we measured the protein levels of ADAM10 using a Western blotting assay 48 h after transfection with either the AS deoxyoligonucleotide or a random deoxyoligonucleotide. The results demonstrated a 2.5-fold and 2.8-fold increase in ADAM10 expression following treatment with the AS deoxyoligonucleotide in HeLa and HEK-APP cells, respectively (Figure 3). Insignificant changes were observed in the deoxyoligonucleotide-free and random control groups. Additionally, RT-PCR was used to assess the

DOI: 10.1021/acs.jmedchem.5b00139
J. Med. Chem. XXXX, XXX, XXX−XXX

Table 2. Binding Data for the Interaction between RNA and the Designed Analogs Using the SPR Assay

	Compound	Ar	SPR (K_D/μM) [a]
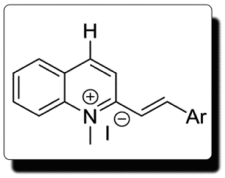	**9**		>50
	10		18.0
	11		9.3
	12		15.9
	13	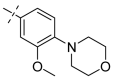	28.2
	14	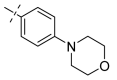	15.8
	15		3.4
	16	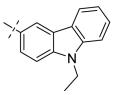	19.2
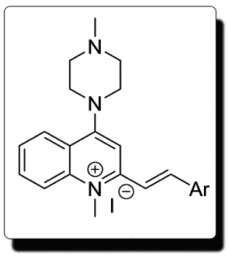	**17**		33.3
	18		11.7
	19		10.9
	20		8.4
	21	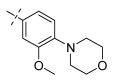	33.0
	22	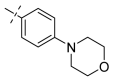	2.6
	23		1.8
	24	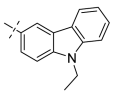	6.1

[a] K_D for different compounds toward the A10-RNA-Wt sequence as determined using SPR. Compounds that did not achieve saturation state at the highest tested concentration (50 μM) are noted. Compounds noted as >50 μM are considered to have low affinity for the RNA QGRS..

changes in the mRNA levels on parallel samples. The results showed no obvious change in the levels of the ADAM10 mRNA (Figure S1 in Supporting Information), indicating that the AS-induced increase in ADAM10 expression was mainly the result of the effects of the deoxyoligonucleotide on the translation process.

Together, our data demonstrated that targeting the QGRS within 5′-UTR of ADAM10 mRNA with a complementary antisense oligonucleotide, an exogenous regulator, could successfully stimulate ADAM10 translation, suggesting that the strategy to use exogenous factors to eliminate the inhibitory effect of the G-quadruplexes in the ADAM10 mRNA on its translation is likely to be feasible.

Initial Screening of RNA QGRS Binders Using SPR. Indeed, antisense-oligonucleotide-based strategies represent sequence-specific modulation for targeting unique RNA G-quadruplex;[25,32] however, their poor pharmacological properties still represent an issue.[29] Thus, "druglike" synthetic small molecules provide an alternative option for targeting RNA G-quadruplex.[31,37] Few previous studies of the use of small

DOI: 10.1021/acs.jmedchem.5b00139
J. Med. Chem. XXXX, XXX, XXX−XXX

Table 3. Binding Data for the Interaction between RNA and Analogs 24−27 Using the SPR Assay

	Compound	R	SPR (K_D/μM) [a]
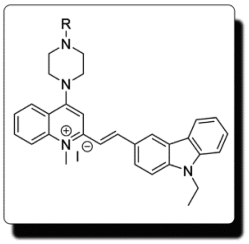	**24**	CH_3	6.1
	25	$(CH_2)_2OH$	32.1
	26	$(CH_2)_2N(CH_3)_2$	>50
	27	$(CH_2)_3N(CH_3)_2$	45.0

[a] K_D for different compounds toward the A10-RNA-Wt sequence as determined using SPR. Compounds that did not achieve saturation state at the highest tested concentration (50 μM) are noted. Compounds noted as >50 μM are considered to have low affinity for the RNA QGRS.

molecules that can bind to the QGRS domains of RNA to enhance gene translation have been reported. To identify small molecules that bind selectively to the QGRS in the 5′-UTR of the ADAM10 mRNA, we performed a screening experiment using surface plasmon resonance (SPR) in which biotinylated wild-type (A10-RNA-Wt) and mutant (A10-RNA-Mut) QGRSs in ADAM10 mRNA were immobilized on a neutravidin-coated sensor chip. SPR is a very sensitive method that measures time-resolved binding events to a surface immobilized biomolecule and provides information on binding kinetics and affinity. In an SPR experiment, a higher relative intensity (RU) indicates a stronger interaction. We tested 7 classes, a total of 52 compounds synthesized by our lab group, including curcumin derivatives, crytolepine derivatives, berberine derivatives, rutaecarpine derivatives, quinazoline derivatives, 1-methylquinolinium derivatives, and natural products. As shown in Figure S2A, it is noteworthy that RU values for three 1-methylquinolinium derivatives (violet bars) for QGRS (A10-RNA-Wt) in ADAM10 were above 50, suggesting their potential high affinity for this domain. Furthermore, the corresponding RU values for the same compounds for the mutant of QGRS were below 20, indicating that the 1-methylquinolinium derivatives had low specific interactions with A10-RNA-Mut (Figure S2B). These results suggested that 1-methylquinolinium might be a class of promising candidates for the development of small molecules that could up-regulate the translation of ADAM10. Encouraged by these results, we proceeded with the development of novel 1-methylquinolinium derivatives by medicinal chemistry optimization.

Synthesis of Methylquinolinium Derivatives. A series of novel 1-methylquinolinium derivatives was developed and synthesized. It was found that the amine side chain at the 4-position and the aromatic ring at the 2-position of the quinoline ring might play important roles in their affinity to the QGRS. Therefore, the newly synthesized compounds were primarily designed with changes in these two positions. The synthesis of the 1-methylquinolinium derivatives (**1**−**28**) was performed following the process shown in Scheme S1 using the method provided in our previous report.[39] Taking into consideration the impact of methylation of the quinoline on the biological activity, four quinoline derivatives (**29**−**32**) were also synthesized according to the method reported by our group (Scheme S2). All of the synthetic compounds (**1**−**32**) are shown in Tables 1−4.

SAR Study Using SPR Assay. To search for more potential RNA QGRS binders, the quinolinium derivatives from the initial screening study and the newly synthesized analogs were further analyzed using the SPR assay to determine the equilibrium dissociation constants (K_D) as indicated by the analysis of the dynamic process of binding, and the structure/binding affinity relationship was explored.

First, to investigate the impact of the amine side chain at the 4-position of 1-methylquinolinium moiety on the binding affinity, two series of analogs that contained a 4-hydroxy-3,5-dimethoxystyryl group (**1**−**4**) or a 2-hydroxy-5-nitrostyryl group (**5**−**8**) at the 2-position of the quinoline were synthesized. The SPR assay results for the binding of these compounds to A10-RNA-Wt (Table 1) showed similar SAR trends, in which the introduction of a morpholine group (**2**, **6**) or a piperidine group (**3**, **7**) had no significant effect on the affinity of compounds to RNA, but the introduction of a methylpiperazine group (**4**, **8**) led to an improvement with K_D values of 16.5 and 16.3 μM, respectively, compared with compounds **1** and **5** (K_D = 20.5 and 46.3 μM, respectively), which lacked substitutions at this position. The results indicated that methylpiperazine motif might be a promising group for the interaction of compounds with QGRS in ADAM10 mRNA and should be maintained in future analogs.

To gain a better understanding of the SAR for the aromatic groups at the 2-position of the quinoline, two series of analogs that either lacked the 4-amino group (**9**−**16**) or contained a 4-methylpiperazine group (**17**−**24**) were designed and synthesized. As shown in Table 2, each series had eight different types of aromatic groups, including substituted phenyl groups, carbazolyl groups, and indolyl groups, which were linked to the 2-position of the quinoline moiety by a vinyl linkage. On the basis of the K_D value results obtained by SPR and shown in Tables 1 and 2, most of compounds in which the 4-amino group was absent (**1**, **5**, **9**−**10**, **12**, **14**−**16**) showed weaker binding abilities than those of analogs containing the 4-methylpiperazine group (**4**, **8**, **17**−**18**, **20**, **22**−**24**). These results further support the significance of the methylpiperazine motif at the 4-position of quinoline. On the other hand, the presence of an aromatic group (Ar) at the 2-position had a notable significant effect on the binding affinity of the compounds to the RNA. A significant enhancement of binding affinity of the compounds to the QGRS of the ADAM10 mRNA was observed (K_D was less than 10 μM) when aromatic

DOI: 10.1021/acs.jmedchem.5b00139
J. Med. Chem. XXXX, XXX, XXX−XXX

Table 4. Binding Data for the Interaction between RNA and Analogs 24 and 28−32 Using the SPR Assay

	Compound	R	Ar	SPR (K_D/μM) [a]
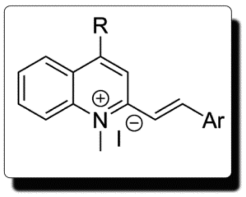	**16**	H	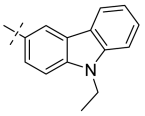	19.2
	22	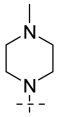	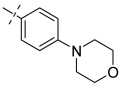	2.6
	24	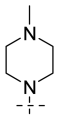	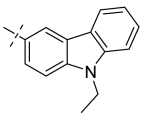	6.1
	28		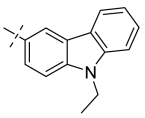	>50
	29	H	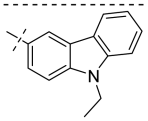	>50
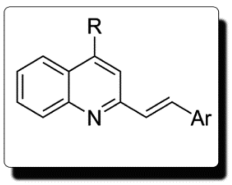	**30**	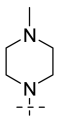	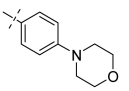	47.6
	31	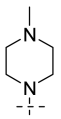	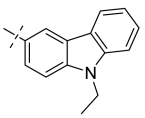	>50
	32		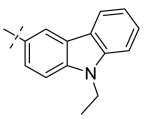	>50

[a] K_D for different compounds toward the A10-RNA-Wt sequence as determined using SPR. Compounds that did not achieve saturation state at the highest tested concentration (50 μM) are noted. Compounds noted as >50 μM are considered to have low affinity for the RNA QGRS.

groups as indolyl (**15**, **23**), *N*-ethylcarbazolyl (**24**), 4-morpholinostyryl (**22**), 4-hydroxylphenyl (**20**), and 3,4,5-trimethoxyphenyl (**11**) groups were present at this position.

The next area for the SAR exploration involved introducing various lengths of side chains into the methylpiperazine group at the 4-position of the quinoline. The SPR results (Table 3) showed that compounds **25**−**27**, which had long side chains at the methylpiperazine group, had weaker binding affinity than the corresponding methylpiperazine analog (**24**), suggesting that a long side chain at the methylpiperazine group at the 4-position of the quinoline was unfavorable for the binding affinity of this class of compounds.

Finally, we explored the significance of a methyl moiety at the 1-position of the quinoline. Four compounds (**29**−**32**) that lacked the 1-methyl group were investigated and compared with those in which this moiety was retained (**16**, **22**, **24**, and **28**). The results shown in Table 4 revealed the necessity of the methyl group at the 1-position of quinoline ring for maintaining binding affinity for RNA QGRS, as indicated by the fact that compounds **29**−**32** were nearly inactive.

None of the above compounds showed any specific interaction with the mutant RNA QGRSs (A10-RNA-Mut) motif in the SPR experiments (data not shown).

Initial Identification of Translational Upregulators of ADAM10 Using the Dual-Luciferase Reporter Assay. Having a high binding affinity for the QGRS of the ADAM10 mRNA is only the first step in identifying compounds that can be used as translation regulators. We next aimed to validate the ability of the QGRS binders to improve translation using the dual-luciferase reporter assay. Dual-luciferase reporter systems are widely used to study the simultaneous expression and measurement of two individual reporter enzymes within a single system. Most of the analogs with high binding affinity were tested using this assay. On the basis of MTT results that all the compounds have no obvious cell toxicity at a concentration of 2 μM (Table S1), dual-luciferase reporter assays[22] were performed initially using a single concentration (2 μM) of the compounds to quickly establish the relative activities of the selected analogs. The data presented in Table 5 show that some of the tested compounds (analogs **15**, **16**, and **22**−**24**) improved the translation efficiency by more than 15%. Notably, treatment with **24** had the most significant effect on enhancing the expression of the *Renilla* luciferase as indicated by its activity (38.3%). On the basis of the selective affinity for the QGRS of the RNA in the SPR experiment and the enhancement effect on the translation efficiency in the dual-

DOI: 10.1021/acs.jmedchem.5b00139
J. Med. Chem. XXXX, XXX, XXX−XXX

Table 5. Change in the Translational Activity for Select Compounds in the Dual-Luciferase Reporter Assay

compd	ratio *Renilla*/firefly luciferase activity[a] (%)
4	108.0 ± 1.3
8	98.7 ± 3.7
9	101.1 ± 2.8
13	101.9 ± 0.3
14	92.0 ± 1.1
15	118.9 ± 2.7
16	116.3 ± 5.2
17	91.5 ± 7.3
22	137.1 ± 0.2
23	115.8 ± 4.3
24	138.3 ± 1.6

[a]2 μM compounds were used in dual-luciferase reporter assays, and the values represent the averages and standard deviations of three independent measurements relative to the no-treatment control.

luciferase reporter assays, we decided to pursue compound **24** as the most potent compound in further studies.

Compound 24 Had a High Affinity for RNA QGRS and a High Capacity To Enhance Translation Activity of a Reporter Gene. To further confirm the binding ability of compound **24** to the QGRS of the ADAM10 mRNA, microscale thermophoresis (MST) and native gel electrophoresis assays were performed. First, the MST technology, which is a contact-free optical and thermodynamic method, is complementary to SPR and it measures the equilibrium dissociation constants (K_d) of compound/RNA interactions in solution at the microliter scale. Consistently, both results of SPR and MST showed high affinity of **24** to QGRS in ADAM10 mRNA with K_D value of 6.1 μM and K_d value of 4.9 μM, respectively (Figure S3). In contrast, **24** bound more weakly to the RNA mutant sequence of ADAM10 mRNA, K_D value of 0.7 M (Figure S3A). Additionally, as shown in Figure 4, increasing the concentration of **24** led to a progressive

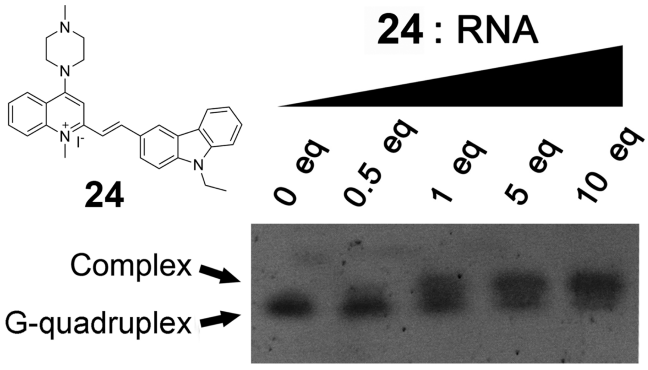

Figure 4. Structures of compound **24** and the binding of **24** to ADAM10 RNA G-quadruplex. Migration of ADAM10 RNA G-quadruplex in the presence of 0, 0.5, 1, 5, 10-fold excess concentrations of **24** in a native 16% polyacrylamide gel.

decrease in the quantity of the RNA G-quadruplex bands (lower bands) and an increase in the RNA–ligand complexes (upper bands) in native gel electrophoresis assays. Consistently, the results of CD spectrum showed that titrating increasing concentrations of compound **24** resulted in a little decrease of the quadruplex secondary structure in the CD signal at 263 nm (Figure S4), reflecting the migration in native gel electrophoresis assays presumably due to its damage of secondary structure of nucleic acids. These combination results suggest the association of **24** with the QGRS of the ADAM10 mRNA in vitro.

To further clarify the capacity of **24** to mitigate translational repression through the QGRS motif, dual-luciferase reporter assays using the three reporter plasmids described previously and RT-PCR were applied. For these experiments, after transfection with the reporter plasmids, the cells were treated with various concentrations of **24** (0, 0.5, 1, 2.5 μM) for 24 h. The cells were inspected prior to the luciferase assay, and no detectable change in the cell number or morphology in any of the treatment groups was observed. We observed a concentration-dependent increase in the *Renilla* luciferase activity (Figure 5A). As shown, 0.5 μM **24** had a moderate effect on translation with an increase of 14.1%. Moreover, when the concentration of **24** was increased to 1 and 2.5 μM, the translation increased by 46.9% and 87.3%, respectively. In contrast, the mutant variant and psi-CHECK-2 blank vector groups showed no obvious effect after treatment with **24** (Figure 5A). The lack of any change in the level of translation of the deletion mutant and mutant variant can be explained by assuming that **24** is specifically interacting with the QGRS in the ADAM10 mRNA in the cells and significantly mitigating the repressive effect of the G-quadruplex on translation. Additionally, no obvious effect was observed (Figure S5) after treatment with an inactive compound **6** (SPR K_D > 50 μM) also confirmed the effect of **24** was derived from its interaction with the QGRS in the ADAM10 mRNA. Interestingly, the results of the RT-PCR assays show very subtle changes in the mRNA levels for both the wild type and mutants (Figure 5B and Figure S6). Since some oncogenes also have QGRS in their 5′-UTR, similar dual-luciferase assays on luciferase reporter plasmid carrying the quadruplex or its mutant sequence of *N-Ras*,[26] *Bcl-2*,[28] and *VEGF*[30] (Figure S7A) were further performed to investigate the specificity of compound **24** among different genes. As shown in Figure S7, **24** had no detectable effect on *VEGF* even at a concentration of 2.5 μM and moderate effect on *N-Ras* and *Bcl-2* with an increase of about 20% (87.3% increase for ADAM10), which indicated the compound **24** had a certain specificity (about 3-fold) to the ADAM10 QGRS.

Given that the G-quadruplex motif is an inhibitory element within the entire context of the ADAM10-5′-UTR,[21,22] to further demonstrate the effect of **24** on ADAM10 translation, we performed additional dual-luciferase reporter assays using a reporter plasmid that carries the entire 5′-UTR (5′UTR-Wt) or its QGRS mutant variant (5′UTR-Mut) in front of the *Renilla* luciferase in the psi-CHECK-2 vector (Figure 2B). The QGRS mutant variant (5′UTR-Mut) was used as system control. As shown in Figure 5C, the relative luciferase activity for the 5′UTR-Wt plasmid increased approximately 9.7% in the presence of 0.5 μM **24**, 22.5% in the presence of 1 μM **24**, and 44.8% when the cells were treated with 2.5 μM **24**. The relative luciferase activity of the mutant variant group showed no obvious change after interaction with **24** (Figure 5C). The RT-PCR results also showed no change in the levels of the luciferase mRNA (Figure 5D and Figure S6) for any of the tested samples, indicating that the gain in activity occurred at the translational level in the cells. These results confirmed that compound **24** could eliminate the translational suppression of the ADAM10 QGRS motif.

DOI: 10.1021/acs.jmedchem.5b00139
J. Med. Chem. XXXX, XXX, XXX−XXX

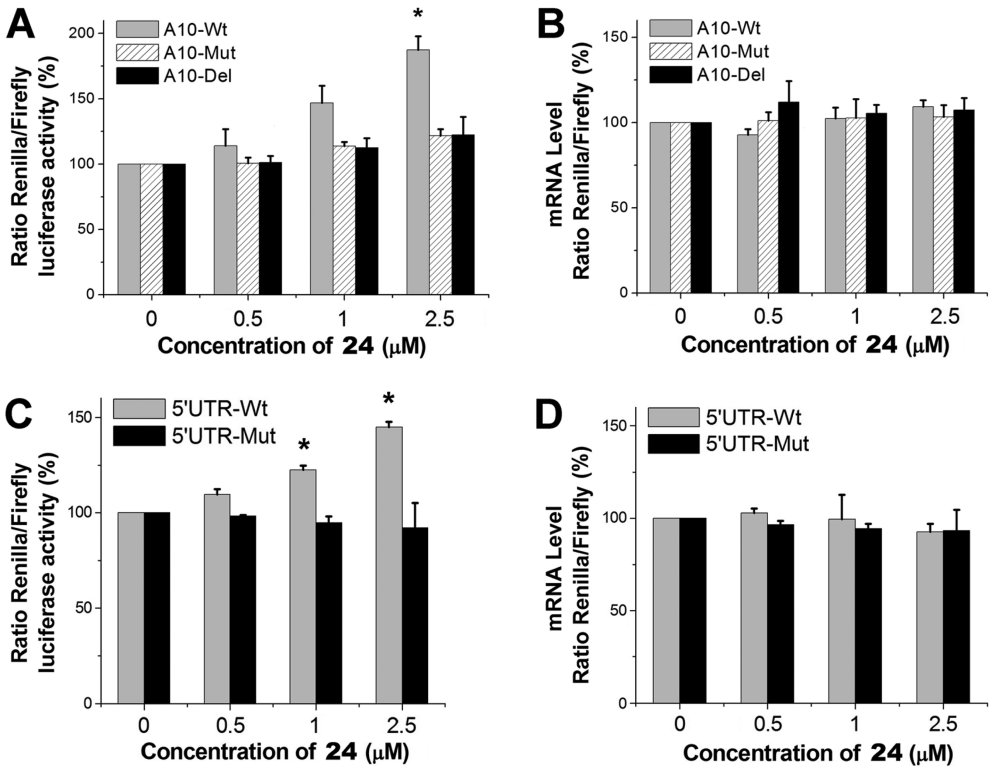

Figure 5. Reporter gene assay results reflect the effect of **24** on the ADAM10 QGRS motif in dual-luciferase assay. (A) Histogram showing the percentage of activity of the translation of the *Renilla* gene as a function of the concentration of **24**. (B) Quantification of the mRNA level of the dual-luciferase reporter gene is shown in Supporting Information Figure S6. (C) Histogram showing the percentage of activity of the translation of the *Renilla* gene as a function of the concentration of **24**. The *Renilla* luciferase activity was normalized to the firefly luciferase activity, and the value for the blank sample in each group was set to 100%. (D) Quantification of the mRNA level of the dual-luciferase reporter gene is shown in Supporting Information Figure S6. For all data, the *Renilla* luciferase activity was normalized to the firefly luciferase activity, and the value for the blank sample in each group was set to 100%. The symbol ∗ indicates a significant difference at $P < 0.05$ vs the ligand-free control (the ligand-free control was set to 1). All data are expressed as the mean ± SD of three independent experiments performed in triplicate.

Compound 24 Efficiently Enhanced ADAM10 Translation and sAPPα Secretion in a Cellular Model. To directly assess the impact of **24** on ADAM10 translation, a further evaluation of the ability of **24** to modulate the translation of the ADAM10 gene in cells was conducted. The protein and mRNA levels of ADAM10 in HEK-APP cells were measured after culturing with 0, 0.5, 0.75, 1, 1.5 μM **24** for 48 h. The results of the Western blotting and RT-PCR assays showed a concentration-dependent increase in the ADAM10 protein levels (20.2%, 55.1%, 76.8%, and 92.9% for treatment with 0.5, 0.75, 1, and 1.5 μM **24**, respectively) (Figure 6A), while only small changes in the mRNA levels of ADAM10 were detected in the **24**-treated cell samples (Figure 6B). It was also found that **24** (it is intrinsically fluorescent) accumulated in the cytoplasm (Figure S8), strongly suggesting that **24** was cell permeable. Moreover, a 3.3-fold increase in the levels of secreted sAPPα, a soluble form of APP cleaved by α-secretase, was detected in the supernatants of the cells that were cultured with 1.5 μM **24** for 48 h (Figure 6A). It is noticeable that for treatment with the ASO the level of sAPPα is lower compared to treatment with compound **24**, to explore the possible causes of this discrepancy, we further detected the impact of **24** on the levels of the APP protein as well as on the α-secretase activity of ADAM10 in vitro. As shown in Figure 6, no obvious impact of **24** on the levels of the APP protein was detected (Figure 6A), but a light increase of the α-secretase activity of ADAM10 was observed (Figure 6C). Thus, the increase of sAPPα in cells might be a combinational result of the increase of ADAM10 protein as well as the enhancement of the α-secretase activity of ADAM10 induced by treatment with compound **24**. The experiment in which Hela cells were cultured with various concentrations of **24** also produced consistent results (Figure S9).

Compound 24 Led to a Decrease in Aβ_{40} Production in HEK-APP Cells. The hallmark of Alzheimer's disease is the significantly elevated Aβ concentrations in cells. We therefore next measured the ability of **24** to reduce the cellular production of Aβ. Because Aβ_{40} constitutes more than 90% of the secretion of Aβ, we measured the change in Aβ_{40} production. HEK-APP cells, which overexpress APP, were treated with increasing concentrations of **24** for 48 h, and the Aβ_{40} production of the cells was quantitatively determined using ELISA assays. As shown in Figure 6D, as expected, **24** was able to inhibit the production of Aβ_{40} in a dose-dependent manner. The production of Aβ_{40} decreased 7.7% in the presence of 0.75 μM **24**, 20.7% in the presence of 1 μM **24**, and 40.8% when the cells were treated with 1.5 μM **24**.

CONCLUSIONS

In this study, 1-methylquinolinium derivatives were identified with favorable predicted ADAM10 mRNA QGRS binding properties. On the basis of these results, a series of 1-methylquinolinium derivatives optimized at the 2- and 4-positions was designed and synthesized to provide valuable insights into the structure−activity relationships of ADAM10 mRNA QGRS binders as well as to screen for translational up-

DOI: 10.1021/acs.jmedchem.5b00139
J. Med. Chem. XXXX, XXX, XXX−XXX

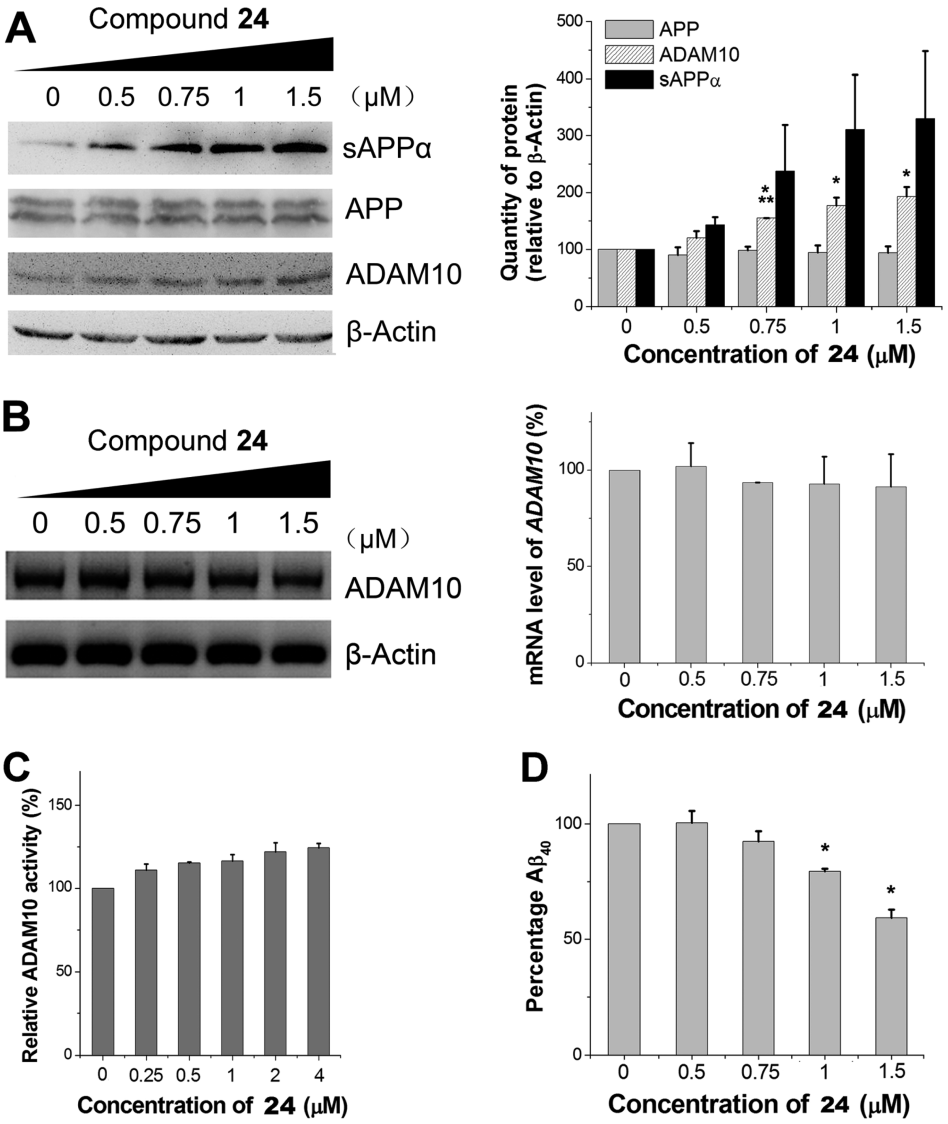

Figure 6. Effect of **24** on HEK-APP cells. HEK-APP cells were treated with various concentrations of **24** for 48 h. (A) Effect of **24** on the protein levels of APP, ADAM10, sAPPα, and β-actin. The results were normalized to β-actin. (B) Effect of **24** on the levels of ADAM10 and β-actin mRNA. The results were normalized to β-actin. (C) Effect of **24** on the α-secretase activity of ADAM10. The ADAM10 protein was treated with various concentrations of **24** for 20 min, and the α-secretase activity of ADAM10 was detected using a fluorogenic peptide substrate. (D) Detection of the effects of **24** on the secretion of Aβ_{40} using an ELISA kit (Invitrogen). All data are expressed as the mean ± SD from three independent experiments. The fold changes in expression were calculated relative to the blank control (the blank control was set to 1). The symbols ∗ and ∗∗∗ indicated significant differences at $P < 0.05$ and $P < 0.001$ vs control.

regulators of ADAM10. The analysis of the in vitro binding properties of the synthesized derivatives by SPR indicated the following aspects of the SAR: (1) the methyl group at the 1-position of quinoline was necessary for the binding to the RNA QGRS sequence, (2) introduction of a methylpiperazine group at the 4-position may enhance the affinity of the compounds for the QGRS, and (3) the type of aromatic groups (Ar) at the 2-position had significant effects on the binding ability of compounds for the target. In particular, several potent ADAM10 mRNA QGRS binders were identified with K_D values in the micromolar range. Further dual-luciferase reporter assays allowed us to identify one carbazolmethylquinolinium analog, compound **24**, as a novel ADAM10 mRNA QGRS binder and translational enhancer. The selected compound **24** was then tested for its ability to enhance ADAM10 translation and sAPPα secretion as well as to decrease Aβ_{40} production by the cells. Our results indicated that using ADAM10 mRNA QGRS binders, such as **24**, is a feasible strategy to up-regulate ADAM10 and thus reduce the formation of Aβ.

Because translation of ADAM10 is suppressed by the G-quadruplexes within its long GC-rich 5′-UTR,[22] in principle there are at least two mechanisms by which **24** targeting of ADAM10 mRNA QGRS could modulate the mRNA translation: (1) by destabilizing the RNA G-quadruplex structure and thus stimulating translation[40,41] or (2) by interfering with a biologically essential RNA G-quadruplex/protein binding event.[29,42] Given that **24** led to a little decrease of the RNA quadruplex secondary structure and had no obvious effect on decreasing the thermodynamic stability of the RNA G-quadruplex in ADAM10 mRNA (data not shown), **24** may interfere with a biologically essential RNA G-quadruplex/protein binding event, including interference with an RNA–translation inhibitor protein or recruitment of a translation initiation protein.

DOI: 10.1021/acs.jmedchem.5b00139
J. Med. Chem. XXXX, XXX, XXX−XXX

Notably, most of the G-quadruplex (G4) motifs in the 5′-UTRs of mRNA have been found to repress translation by approximately 50%, suggesting that functional proteins exist to maintain the equilibrium of the folded state in which the G-quadruplex is formed and translation is prevented. Recently, the first systematic approach to identifying proteins that bind to G-quadruplex elements in 5′-UTRs of mRNAs using pull-down assays and MALDI-TOF MS was published.[43] The interaction between the cellular proteins and the G-quadruplexes located in two mRNAs (*MMP16* and *ARPC2*) was investigated. Furthermore, a selective mechanism for the translational control associated with the G4 motifs in the 5′-UTRs has been elucidated. In another study, elf4A was demonstrated to be required for the translation of mRNAs containing G-quadruplexes in their 5′-UTRs.[44]

Some reports have characterized small molecules that modulate the DNA G-quadruplex/protein binding event.[45,46] However, there have been fewer developments in the field of functional RNA G-quadruplex ligands. Recently, Zamiri et al. showed the cationic porphyrin TMPyP4 bound to the $_r(GGGGCC)_8$ RNA of the *C9orf72* gene and blocked interaction with RNA-binding proteins.[47] On the basis of the previous research that identified several proteins, including ASF/SF2 and hnRNPA, that selectively bind to the $_r(GGGGCC)_8$ RNA in vivo,[48,49] the authors found that TMPyP4 disrupted the binding of ASF/SF2 and hnRNPA1 to $_r(GGGGCC)_8$, suggesting that this may be a viable avenue for the development of therapeutic treatments. Thus, further studies are needed to confirm the speculation that compound **24** can enhance the translation of ADAM10 via binding to the RNA G-quadruplexes and interfering with a biologically essential RNA G4/protein binding event.

Our study provided new insight into the design and discovery of an RNA QGRS binder and proposed a new molecular strategy by which interactions of these molecules with RNA QGRS may modulate translation of ADAM10.

EXPERIMENTAL SECTION

General Methods. ^{1}H and ^{13}C NMR spectra were recorded using TMS as the internal standard in DMSO-d_6 or $CDCl_3$ with a Bruker BioSpin GmbH spectrometer at 400 and 100 MHz, respectively. The chemical shifts are reported in parts per million (ppm) relative to residual $CHCl_3$ (δ = 7.26, ^{1}H; δ = 77.0, ^{13}C) and DMSO (δ = 2.50, ^{1}H; δ = 39.5, ^{13}C) in the corresponding deuterated solvents. The mass spectra (MS) were recorded on a Shimadzu LCMS-2010A instrument with an ESI or ACPI mass-selective detector, and high-resolution mass spectra (HRMS) were obtained using a Shimadzu LCMS-IT-TOF instrument. The melting points (Mp) were determined using an SRS-OptiMelt automated melting point instrument without correction. Flash column chromatography was performed with silica gel (200−300 mesh) purchased from Qingdao Haiyang Chemical Co. Ltd. The purities of the synthesized compounds were confirmed to be higher than 95% by analytical HPLC performed using a dual pump Shimadzu LC-20AB system equipped with an Ultimate XB-C18 column and eluted with methanol/water (80%) containing 0.1% TFA at a flow rate of 0.2 mL min^{-1}. Aniline, ethyl acetoacetate, polyphosphoric acid, $POCl_3$, ethanol, *n*-butanol, 1,4-dioxane, THF, and all the amines were commercially available.

Synthesis of Intermediates. The intermediates **1a**, **2a**, **3a**, and **3b** were prepared following the process shown in Scheme S1 using the method by our previous report.[39]

1-*N*-Methyl-2-methylquinolinium Iodode (4a). The preparation was according to the synthetic method of intermediates **3a** and **3b**. ^{1}H NMR (400 Hz, DMSO-d_6): δ 9.11 (d, 1H, J = 8.0), 8.60−8.57 (dd, 1H, J = 4.0, J = 8.0), 8.41−8.38(dd, 1H, J = 4.0, J = 4.0), 8.23−8.19 (m, 1H), 8.13 (d, 1H, J = 8.0), 7.99−7.95 (m, 1H), 4.45 (s, 3H), 3.10 (s, 3H). ^{13}C NMR (100 Hz, DMSO-d_6): δ 161.1, 145.3, 135.0, 128.9, 125.1, 119.0, 39.9, 23, 3.

General Procedure A: Preparation of Compounds 6a and 6b. A suspension of compound **2a** (1.77 g, 10 mmol), alicyclic amine (20 mmol), and *p*-toluenesulfonic acid (0.60 g, 3.2 mmol) was stirred under reflux for 10 h. After completion of the reaction, the reaction mixture was cooled to room temperature, poured into ice−water (100 mL), and then aqueous NaOH was added to make the solution basic. The mixture was extracted with three 50 mL portions of CH_2Cl_2. The combined organic phase was washed with 40 mL of water, dried over magnesium sulfate, and concentrated under reduced pressure. The crude product was purified by using flash column chromatography to give **6a** and **6b**.

4-(*N*-Methylpiperazin-1-yl)-2-methylquinoline (6a). Compound **2a** was reacted with *N*-methylpiperazine according to general procedure A to afford **6a** as pale yellow liquid in 75% yield. ^{1}H NMR (400 MHz, $CDCl_3$): δ 7.98 (t, J = 8.0 Hz, 2H), 7.62 (t, J = 8.0 Hz, 1H), 7.42 (t, J = 8.0 Hz, 1H), 6.74 (s, 1H), 3.27 (s, 4H), 2.73 (s, 4H), 2.69 (s, 3H), 2.43 (s, 3H).

4-(Piperidin-1-yl)-2-methylquinoline (6b). Compound **2a** was reacted with piperidine according to general procedure A to afford **6b** as a white solid in 64% yield. Mp 41.2−42.6 °C. ^{1}H NMR (400 MHz, $CDCl_3$): δ 7.95 (d, J = 8.0 Hz, 2H), 7.59 (t, J = 8.0 Hz, 1H), 7.40 (t, J = 8.0 Hz, 1H), 6.71 (s, 1H), 3.15 (s, 4H), 2.66 (s, 3H), 1.84 (s, 4H), 1.68(s, 2H). ^{1}H NMR (400 MHz, $CDCl_3$): δ 7.95 (d, J = 8.0 Hz, 2H), 7.59 (t, J = 8.0 Hz, 1H), 7.40 (t, J = 8.0 Hz, 1H), 6.71 (s, 1H), 3.15 (s, 4H), 2.66 (s, 3H), 1.84 (s, 4H), 1.68 (s, 2H).

General Procedure B: Preparation of (2-Aromatic vinyl)-1-*N*-methylquinolinium Derivatives 1−28. A suspension of **3a** and **3b** (0.65 g, 0.2 mmol), aromatic aldehydes (0.2 mmol, 1.0 equiv amount), 1.5 equiv amount secondary amine, and 15 mL of ethanol was heated in a flask or sealed tube for 3 h at 80 °C. A precipitate was formed during the process of the reaction. The reaction mixture was allowed to cool to room temperature. The flask or sealed tube was then placed in an ice bath, and the solution was filtered and washed thoroughly with anhydrous ethanol to afford the (2-aromatic vinyl)-1-*N*-methylquinolinium derivatives.

(*E*)-2-(4-Hydroxy-3,5-dimethoxystyryl)-1-methylquinolin-1-ium Iodide (1). Following general procedure B for (2-aromatic vinyl)-1-*N*-methylquinolinium derivatives, the product was obtained as a green-yellow solid. Mp > 200 °C.^{1}H NMR (400 Hz, DMSO-d_6): δ 9.42 (s, 1H), 8.99 (d, 1H, J = 8.0), 8.54 (d, 2H, J = 8.0), 8.32 (d, 1H, J = 8.0), 8.18 (d, 1H, J = 16.0), 8.15 (d, 1H, J = 8.0), 7.93 (t, 1H, J = 8.0), 7.76 (d, 1H, J = 16.0), 7.32 (s, 2H), 4.56 (s, 3H), 3.90 (s, 6H). ^{13}C NMR (100 MHz, DMSO-d_6): δ 156.4, 148.5, 148.2, 143.3, 140.1, 139.2, 134.6, 129.9, 128.6, 127.4, 125.4, 120.6, 119.2, 115.7, 107.6, 56.3, 18.5. Purity: 99.8% by HPLC. ESI-HRMS ($C_{20}H_{20}NO_3$): calcd, 322.1438 [M]$^+$; found, 322.1446.

(*E*)-2-(4-Hydroxy-3,5-dimethoxystyryl)-1-methyl-4-morpholinoquinolin-1-ium Iodide (2). Following general procedure B for (2-aromatic vinyl)-1-*N*-methylquinolinium derivatives, the product was obtained as a green-yellow solid. Mp > 200 °C. ^{1}H NMR (400 Hz, DMSO-d_6): δ 9.15 (s, 1H), 8.32 (d, 1H, J = 8.0), 8.20 (d, 1H, J = 8.0), 8.04 (t, 1H, J = 8.0), 7.85 (d, 1H, J = 16.0), 7.75 (t, 1H, J = 8.0), 7.59 (d, 1H, J = 16.0), 7.49(s, 1H), 7.20 (s, 2H), 4.27 (s, 3H), 3.91 (s, 4H), 3.88 (s, 6H), 3.77 (s, 4H). ^{13}C NMR (100 MHz, DMSO-d_6): δ 159.3, 154.5, 148.1, 144.5, 140.8, 138.9, 133.7, 126.5, 126.3, 125.6, 119.7, 119.3, 116.6, 106.8, 105.0, 65.8, 56.3, 52.0, 38.3. Purity: 99.0% by HPLC. ESI-HRMS ($C_{24}H_{27}N_2O_4$): calcd, 407.1965 [M]$^+$; found, 407.1945.

(*E*)-2-(4-Hydroxy-3,5-dimethoxystyryl)-1-methyl-4-(piperidin-1-yl)quinolin-1-ium Iodide (3). Following general procedure B for (2-aromatic vinyl)-1-*N*-methylquinolinium derivatives, the product was obtained as a green-yellow solid. Mp > 200 °C. ^{1}H NMR (400 Hz, DMSO-d_6): δ 8.17 (d, 1H, J = 8.0), 8.03 (d, 1H, J = 8.0), 7.94 (t, 1H, J = 8.0), 7.80 (d, 1 H, J = 16.0), 7.65 (t, 1H, J = 8.0), 7.35 (s, 1H), 7.31 (d, 1H, J = 16.0), 7.15 (s, 2H), 4.14 (s, 3H), 3.83 (s, 6H), 3.62 (s, 4H), 1.82 (s, 4H), 1.74 (s, 2H),1.53 (s, 1H). ^{13}C NMR (100 MHz, DMSO-d_6): δ 158.7, 153.8, 148.6, 144.0, 140.8, 133.2, 126.2, 125.5, 123.7,

DOI: 10.1021/acs.jmedchem.5b00139
J. Med. Chem. XXXX, XXX, XXX−XXX

119.7, 118.8, 113.8, 108.6, 107.2, 104.4, 56.2, 44.5, 37.8, 25.4, 23.5. Purity: 98.8% by HPLC. ESI-HRMS ($C_{25}H_{29}N_2O_3$): calcd, 405.2173 $[M]^+$; found, 405.2141.

(*E*)-2-(4-Hydroxy-3,5-dimethoxystyryl)-1-methyl-4-(4-methylpiperazin-1-yl)quinolin-1-ium Iodide (4). Following general procedure B for (2-aromatic vinyl)-1-*N*-methylquinolinium derivatives, the product was obtained as a green-yellow solid. Mp > 200 °C. ^{1}H NMR (400 Hz, DMSO-d_6): δ 8.30 (d, 1H, J = 8.0), 8.14 (d, 1H, J = 7.2), 8.03 (s, 1H), 7.89 (d, 1H, J = 16.0), 7.75 (s, 1H), 7.58 (d, 1H, J = 16.0), 7.50 (s, 1H), 7.23 (s, 2H), 4.26 (s, 3H), 3.87 (s, 6H), 3.80 (s, 4H), 2.75 (s, 4H), 2.39 (s, 3H). ^{13}C NMR (100 MHz, DMSO-d_6): δ 159.2, 154.4, 148.1, 144.4, 140.7, 138.8, 133.7, 126.5, 126.3, 125.6, 119.7, 119.3, 116.6, 106.8, 105.1, 56.4, 54.0, 51.2, 45.1, 38.3. Purity: 99.7% by HPLC. ESI-HRMS ($C_{25}H_{30}N_3O_3$): calcd, 420.2282 $[M]^+$; found, 420.2274.

(*E*)-2-(2-Hydroxy-5-nitrostyryl)-1-methylquinolin-1-ium Iodide (5). Following general procedure B for (2-aromatic vinyl)-1-*N*-methylquinolinium derivatives, the product was obtained as a green-yellow solid. Mp > 200 °C. ^{1}H NMR (400 Hz, DMSO-d_6): δ 8.82−8.80 (m, 2H), 8.49 (d, 1H, J = 12.0), 8.36 (s, 2H), 8.22 (d, 2H, J = 8.0), 8.06 (t, 1H, J = 8.0), 7.84−7.79 (m, 2H), 6.26 (d, 1H, J = 12.0), 4.36 (s, 3H). ^{13}C NMR (100 MHz, DMSO-d_6) δ 179.1, 157.8, 148.5, 141.2, 138.9, 133.6, 131.9, 130.2, 129.4, 127.4, 126.9, 126.4, 123.0, 121.4, 119.7, 118.2, 113.5, 38.2. Purity: 98.8% by HPLC. ESI-HRMS ($C_{18}H_{15}N_2O_3$): calcd, 307.1077 $[M]^+$; found, 307.1092.

(*E*)-2-(2-Hydroxy-5-nitrostyryl)-1-methyl-4-morpholinoquinolin-1-ium Iodide (6). Following general procedure B for (2-aromatic vinyl)-1-*N*-methylquinolinium derivatives, the product was obtained as a green-yellow solid. Mp > 200 °C. ^{1}H NMR (400 Hz, DMSO-d_6): δ 8.65 (d, 1H, J = 12.0), 8.34 (d, 1H, J = 4.0), 8.23 (d, 1H, J = 8.0), 8.15 (d, 1H, J = 8.0), 7.99 (t, 1H, J = 8.0), 7.92 (d, 1H, J = 16.0), 7.80 (dd, 1H, J = 4.0, J = 8.0), 7.70 (t, 1H, J = 8.0), 7.51 (s, 1H), 6.26 (d, 1H, J = 8.0), 4.16 (s, 3H), 3.91 (t, 4H, J = 4.0), 3.69 (t, 4H, J = 4.0). ^{13}C NMR (100 MHz, DMSO-d_6) δ 158.9, 156.1, 143.7, 140.7, 133.5, 131.4, 130.9, 126.8, 126.3, 126.1, 122.1, 121.7 119.8, 119.1, 116.8, 104.6, 99.6, 65.9, 52.0, 37.8. Purity: 97.7% by HPLC. ESI-HRMS ($C_{22}H_{22}N_3O_4$): calcd, 392.1605 $[M]^+$; found, 392.1592.

(*E*)-2-(2-Hydroxy-5-nitrostyryl)-1-methyl-4-(piperidin-1-yl)-quinolin-1-ium Iodide (7). Following general procedure B for (2-aromatic vinyl)-1-*N*-methylquinolinium derivatives, the product was obtained as a green-yellow solid. Mp > 200 °C. ^{1}H NMR (400 Hz, DMSO-d_6): δ 8.66 (d, 1H, J = 12.0), 8.30 (d, 1H, J = 4.0), 8.18 (d, 1H, J = 12.0), 8.06 (d, 1H, J = 8.0), 7.96 (t, 1H, J = 8.0), 7.87 (d, 1H, J = 16.0), 7.80 (m, 1H), 6.69 (t, 1H, J = 8.0), 7.44 (s, 1H), 6.16 (d, 1H, J = 8.0), 4.13 (s, 3H), 3.65 (t, 4H, J = 4.0), 1.83 (s, 4H), 1.75 (s, 2H). ^{13}C NMR (100 MHz, DMSO-d_6) δ 179.3, 158.9, 156.1, 144.2, 140.5, 132.9, 131.2, 129.1, 126.4, 125.9, 125.3, 122.4, 121.6, 119.8, 118.5, 115.1, 103.7, 52.4, 37.1, 25.1, 23.2. Purity: 95.2% by HPLC. ESI-HRMS ($C_{23}H_{24}N_3O_3$): calcd, 390.1812 $[M]^+$; found, 390.1815.

(*E*)-2-(2-Hydroxy-5-nitrostyryl)-1-methyl-4-(4-methylpiperazin-1-yl)quinolin-1-ium Iodide (8). Following general procedure B for (2-aromatic vinyl)-1-*N*-methylquinolinium derivatives, the product was obtained as a green-yellow solid. Mp > 200 °C. ^{1}H NMR (400 Hz, DMSO-d_6): δ 8.58 (s, 1H), 8.29 (d, 1H, J = 12.0), 8.17 (s, 1H), 8.14 (d, 1H, J = 12.0), 8.09 (d, 1H, J = 8.0), 8.06 (t, 1H, J = 8.0), 7.88 (d, 1H, J = 16.0), 7.75(t, 1H, J = 8.0), 7.50 (s, 1H), 6.92 (d, 1H, J = 8.0), 4.20 (s, 3H), 3.85 (s, 4H), 2.83 (s, 4H), 2. 54 (s, 3H). ^{13}C NMR (100 MHz, DMSO-d_6) δ 159.2, 154.7, 140.7, 139.2, 136.8, 133.9, 127.5, 126.9, 126.6, 126.4, 122.3, 120.9, 119.7, 119.2, 118.4, 105.4, 99.6, 53.6, 50.7, 44.6, 38.2. Purity: 95.4% by HPLC. ESI-HRMS ($C_{23}H_{25}N_4O_3$): calcd, 405.1921 $[M]^+$; found, 405.1908.

(*E*)-1-Methyl-2-styrylquinolin-1-ium Iodide (9). Following general procedure B for (2-aromatic vinyl)-1-*N*-methylquinolinium derivatives, the product was obtained as a green-yellow solid. Mp > 200 °C. ^{1}H NMR (400 Hz, DMSO-d_6): 9.13 (d, 1H, J = 8.0), 8.61 (t, 2H, J = 8.0), 8.40 (t, 1H, J = 8.0), 8.25−8.20 (m, 2H), 8.02−7.96 (m, 4H), 7.55 (s, 3H), 4.60 (s, 3H). ^{13}C NMR (100 MHz, DMSO-d_6): δ 156.2, 146.7, 144.3, 139.2, 135.0, 134.8, 131.3, 130.1, 129.1, 127.9, 121.3, 119.5, 119.4, 48.6. Purity: 98.8% by HPLC. ESI-HRMS ($C_{18}H_{16}N$): calcd, 246.1277 $[M]^+$; found, 246.1286.

(*E*)-2-(4-Fluoro-3-methoxystyryl)-1-methylquinolin-1-ium (10). Following general procedure B for (2-aromatic vinyl)-1-*N*-methylquinolinium derivatives, the product was obtained as a green-yellow solid. Mp > 200 °C. ^{1}H NMR (400 Hz, DMSO-d_6): δ 9.12 (d, 1H, J = 8.0), 8.59 (t, 2H, J = 8.0), 8.39 (d, 1H, J = 4.0), 8.22−8.18 (m, 2H), 8.00−7.92 (m, 2H), 7.81 (d, 1H, J = 8.0), 7.57 (t, 1H, J = 4.0), 7.41−7.37 (m, 1H), 4.62 (s, 3H), 3.99 (s, 3H). ^{13}C NMR (100 MHz, DMSO-d_6) δ 156.1, 152.1, 147.6, 146.0, 144.3, 139.2, 135.0, 132.0, 130.0, 129.1, 127.8, 123.3, 121.2, 119.4, 119.3, 116.6, 116.4, 113.6, 72.6, 56.5, 40.2. Purity: 98.4% by HPLC. ESI-HRMS ($C_{19}H_{17}NOF$): calcd, 294.1289 $[M]^+$; found, 294.1285.

(*E*)-1-Methyl-2-(3,4,5-trimethoxystyryl)quinolin-1-ium Iodide (11). Following general procedure for (2-aromatic vinyl)-1-*N*-methylquinolinium derivatives, the product was obtained as a green-yellow solid. Mp > 200 °C. ^{1}H NMR (400 Hz, DMSO-d_6): δ 9.08 (d, 1H, J = 8.0), 8.58 (d, 1H, J = 12.0), 8.55 (d, 1H, J = 12.0), 8.36 (d, 1H, J = 12.0), 8.21 (d, 1H, J = 8.0), 8.17 (d, 1H, J = 16.0), 7.79 (t, 1H, J = 8.0), 7.79 (d, 1H, J = 16.0), 7.33 (s, 2H), 4.60 (s, 3H), 3.91 (s, 6H), 3.77 (s, 3H). ^{13}C NMR (100 MHz, DMSO-d_6) δ 158.9, 156.1, 143.7, 140.7, 133.5, 131.4, 130.9, 126.8, 126.3, 126.1, 122.1, 121.7, 119.8, 119.1, 116.8, 104.6, 99.6, 65.9, 52.0, 37.8. Purity: 99.8% by HPLC. ESI-HRMS ($C_{21}H_{22}NO_3$): calcd, 336.1594 $[M]^+$; found, 336.1594.

(*E*)-2-(4-Hydroxystyryl)-1-methylquinolin-1-ium Iodide (12). Following general procedure B for (2-aromatic vinyl)-1-*N*-methylquinolinium derivatives, the product was obtained as a green-yellow solid. Mp > 200 °C. ^{1}H NMR (400 Hz, DMSO-d_6): δ 10.37 (s, 1H), 8.98 (d, 1H, J = 8.0), 8.56 (d, 1H, J = 8.0), 8.52 (d, 1H, J = 16.0), 8.32 (d, 1H, J = 8.0), 8.21 (d, 1H, J = 16.0), 8.16 (t, 1H, J = 8.0), 7.92 (t, 1H, J = 8.0), 7.88 (d, 2H, J = 8.0), 7.71 (d, 1H, J = 16.0), 6.93 (d, 2H, J = 8.0), 4.53 (s, 3H). ^{13}C NMR (100 MHz, DMSO-d_6) δ 161.1, 156.2, 147.6, 143.1, 138.9, 134.5, 131.7, 129.8, 128.5, 127.2, 126.1, 120.6, 119.0, 116.0, 115.1, 39.8. Purity: 99.8% by HPLC. ESI-HRMS ($C_{18}H_{16}NO$): calcd, 262.1226 $[M]^+$; found, 262.1236.

(*E*)-2-(3-Methoxy-4-morpholinostyryl)-1-methylquinolin-1-ium Iodide (13). Following general procedure B for (2-aromatic vinyl)-1-*N*-methylquinolinium derivatives, the product was obtained as a green-yellow solid. Mp > 200 °C. ^{1}H NMR (400 Hz, DMSO-d_6): δ 9.00 (d, 1H, J = 8.0), 8.55 (t, 2H, J = 12.0), 8.33 (d, 1H, J = 8.0), 8.23 (d, 1H, J = 16.0), 8.16 (t, 1H, J = 6.0), 7.93 (t, 1H, J = 8.0), 7.79 (d, 1H, J = 16.0), 7.59 (s, 1H), 7.52 (d, 1H, J = 8.0), 7.00 (d, 1H, J = 8.0), 4.56 (s, 3H), 3.94 (s, 3H), 3.75 (s, 4H), 3.14 (s, 4H). ^{13}C NMR (100 MHz, DMSO-d_6): δ 156.3, 151.6, 147.7, 144.5, 143.3, 139.2, 134.6, 129.9, 128.7, 128.7, 127.4, 124.7, 120.8, 119.2, 117.5, 116.2, 111.5, 66.1, 55.9, 50.0, 39.4. Purity: 98.6% by HPLC. ESI-HRMS ($C_{23}H_{25}N_2O_2$: calcd, 361.1911 $[M]^+$; found, 361.1893.

(*E*)-1-Methyl-2-(4-morpholinostyryl)quinolin-1-ium Iodide (14). Following general procedure B for (2-aromatic vinyl)-1-*N*-methylquinolinium derivatives, the product was obtained as a green-yellow solid. Mp > 200 °C. ^{1}H NMR (400 Hz, DMSO-d_6): δ 8.90 (d, 1H, J = 8.0), 8.53 (t, 1H, J = 8.0), 8.47 (t, 1H, J = 8.0), 8.29−8.25 (m, 2H), 8.22 (d, 1H, J = 4.0), 8.14−8.09 (m, 2H), 7.89 (d, 1H, J = 16.0), 7.67 (d, 1H, J = 4.0), 7.07 (d, 2H, J = 8.0), 4.49 (s, 3H), 3.76 (d, 4H), 3.36 (s, 4H). ^{13}C NMR (100 MHz, DMSO-d_6): δ 156.3, 153.2, 148.1, 142.6, 139.2, 134.3, 131.5, 129.8, 128.3, 127.1, 124.7, 120.4, 119.0, 113.8, 113.8, 65.8, 46.7, 39.1. Purity: 98.9% by HPLC. ESI-HRMS ($C_{22}H_{23}N_2O$): calcd, 331.1805 $[M]^+$; found, 331.1809.

(*E*)-2-(2-(1*H*-Indol-2-yl)vinyl)-1-methylquinolin-1-ium Iodide (15). Following general procedure B for (2-aromatic vinyl)-1-*N*-methylquinolinium derivatives, the product was obtained as a green-yellow solid. Mp > 200 °C. ^{1}H NMR (400 Hz, DMSO-d_6): δ 12.29 (s, 1H), 8.80 (d, 1H, J = 8.0), 8.64 (d, 1H, J = 16.0), 8.59 (d, 1H, J = 8.0), 8.40 (t, 2H, J = 12.0), 8.22 (t, 2H, J = 8.0), 8.07 (t, 1H, J = 8.0), 7.84 (d, 1H, J = 8.0), 7.53 (t, 2H, J = 8.0), 7.30 (s, 2H), 4.46 (s, 3H). ^{13}C NMR (100 MHz, DMSO-d_6): δ 156.6, 142.8, 141.6, 139.1, 137.5, 134.5, 134.0, 129.7, 127.8, 126.6, 125.2, 123.4, 121.9, 120.3, 119.8, 118.7, 114.5, 112.8, 111.4, 38.9. Purity: 98.8% by HPLC. ESI-HRMS ($C_{20}H_{17}N_2$): calcd, 285.1386 $[M]^+$; found, 285.1391.

(*E*)-2-(2-(9-Ethyl-9*H*-carbazol-2-yl)vinyl)-1-methyl-quinolin-1-ium Iodide (16). Following general procedure B for (2-aromatic vinyl)-1-*N*-methylquinolinium derivatives, the product was obtained as

DOI: 10.1021/acs.jmedchem.5b00139
J. Med. Chem. XXXX, XXX, XXX−XXX

a green-yellow solid. Mp > 200 °C. ^{1}H NMR (400 Hz, DMSO-d_6): δ 8.95 (d, 1H, J = 8.0), 8.87 (s, 1H), 8.61 (d, 1H, J = 8.0), 8.49 (t, 2H, J = 8.0), 8.30−8.24(m, 2H), 8.13 (t, 2H, J = 8.0), 7.96−7.88 (m, 2H), 7.78 (dd, 2H, J = 8.0, J = 12.0), 7.54 (t, 1H, J = 8.0), 7.33 (t, 1H, J = 8.0), 4.58 (s, 3H), 4.50 (d, 2H, J = 8.0), 1.36 (s, 3H). ^{13}C NMR (100 MHz, DMSO-d_6): δ 156.1, 149.0, 142.8, 141.5, 140.1, 138.9, 134.3, 129.7, 128.3, 127.9, 127.0, 126.6, 126.0, 122.7, 122.4, 122.1, 120.6, 120.4, 119.8, 118.8, 115.2, 109.8, 109.7, 39.6, 37.3, 13.8. Purity: 99.5% by HPLC. ESI-HRMS ($C_{26}H_{23}N_2$): calcd, 363.1856 [M]$^+$; found, 363.1866.

(*E*)-1-Methyl-4-(4-methylpiperazin-1-yl)-2-styrylquinolin-1-ium Iodide (17). Following general procedure B for (2-aromatic vinyl)-1-*N*-methylquinolinium derivatives, the product was obtained as a green-yellow solid. Mp > 200 °C. ^{1}H NMR (400 Hz, DMSO-d_6): δ 8.32−8.28 (m, 1H), 8.18−8.15 (m, 1H), 8.04 (t, 1H, J = 12.0), 7.92−7.85 (m, 3H), 7.76−7.71 (m, 2H), 7.99 (d, 1H, J = 8.0), 7.50 (s, 4H), 4.24 (s, 3H), 3.84 (s, 4H), 2.65 (s, 4H), 2.32 (s, 3H). ^{13}C NMR (100 MHz, DMSO-d_6) δ 159.5, 153.7, 142.6, 140.8, 135.1, 133.8, 132.6, 130.3, 129.2, 128.9, 128.4, 126.7, 126.2, 120.2, 119.5, 119.2, 105.2, 54.2, 51.6, 45.4, 38.3. Purity: 96.1% by HPLC. ESI-HRMS ($C_{23}H_{26}N_3$): calcd, 344.2121 [M]$^+$; found, 344.2115.

(*E*)-2-(4-Fluoro-3-methoxystyryl)-1-methyl-4-(4-methylpiperazin-1-yl) quinolin-1-ium Iodide (18). Following general procedure B for (2-aromatic vinyl)-1-*N*-methylquinolinium derivatives, the product was obtained as a green-yellow solid. Mp > 200 °C. ^{1}H NMR (400 Hz, DMSO-d_6): δ 8.30 (d, 1H, J = 8.0), 8.15 (d, 1H, J = 8.0), 8.04 (t, 1H, J = 8.0), 7.83 (d,1H, J = 20.0), 7.78 (d, 1H, J = 16.0), 7.74 (s, 1H), 7.70−7.68 (m, 1H),7.46 (s, 2H), 7.34 (t, 1H, J = 12.0), 4.24 (s, 3H), 3.95 (s, 3H), 3.82 (s, 4H), 2.61 (s, 4H), 2.29(s, 2H). ^{13}C NMR (100 MHz, DMSO-d_6) δ 159.4, 153.9, 153.6, 151.4, 147.5, 147.3, 141.8, 140.7, 133.8, 132.2, 126.6, 126.2, 122.1, 120.0, 119.4, 119.2, 116.3, 116.1, 113.3, 105.3, 56.5, 54.3, 51.7, 45.4, 38.5. Purity: 95.3% by HPLC. ESI-HRMS ($C_{24}H_{27}N_3OF$): calcd, 392.2133 [M]$^+$; found, 392.2114.

(*E*)-1-Methyl-4-(4-methylpiperazin-1-yl)-2-(3,4,5-trimethoxystyryl)quinolin-1-ium Iodide (19). Following general procedure B for (2-aromatic vinyl)-1-*N*-methylquinolinium derivatives, the product was obtained as a green-yellow solid. Mp > 200 °C. ^{1}H NMR (400 Hz, $CDCl_3$): δ 8.00−7.88 (m, 4H), 7.71 (d, 1H, J = 16.0), 7.64−7.61 (m, 1H), 7.41 (s, 1H), 7.21 (s, 2H), 4.37 (s, 3H), 3.93 (m, 4H), 3.91 (s, 6H), 3.75 (s, 3H), 2.76 (m, 4H), 2.41 (s, 3H). ^{13}C NMR (100 Hz, $CDCl_3$): δ 159.7, 155.1, 153.1, 144.8, 141.2, 140.0, 134.3, 130.2, 126.7, 126.1, 118.6, 118.4, 106.7, 106.1, 60.8, 57.4, 54.7, 52.4, 45.8, 40.4. Purity: 99.4% by HPLC. ESI-HRMS ($C_{26}H_{32}N_3O_3$): calcd, 434.2438 [M]$^+$; found, 434.2411.

(*E*)-2-(4-Hydroxystyryl)-1-methyl-4-(4-methylpiperazin-1-yl)-quinolin-1-ium Iodide (20). Following general procedure B for (2-aromatic vinyl)-1-*N*-methylquinolinium derivatives, the product was obtained as a green-yellow solid. Mp > 200 °C. ^{1}H NMR (400 Hz, DMSO-d_6): δ 8.29 (d, 1H, J = 8.0), 8.14 (d, 1H, J = 8.0), 8.02 (t, 1H, J = 8.0), 7.85 (d, 1H, J = 16.0), 7.75 (m, 3H), 7.49 (m, 2H), 6.90 (d, 2H, J = 8.0), 4.22 (s, 3H), 3.79 (s, 4H), 2.68 (s, 4H), 2.34 (s, 3H). ^{13}C NMR (100 Hz, DMSO-d_6): δ 160.0, 159.1, 154.3, 143.6, 140.6, 133.6, 130.7, 126.4, 126.3, 126.2, 119.6, 119.1, 116.0, 115.8, 105.0, 54.0, 51.3, 45.1, 42.8. Purity: 97.2% by HPLC. ESI-HRMS ($C_{23}H_{26}N_3O$): calcd, 360.2070 [M]$^+$; found, 360.2083.

(*E*)-2-(3-Methoxy-4-morpholinostyryl)-1-methyl-4-(4- methylpiperazin-1-yl)quinolin-1-ium Iodide (21). Following general procedure B for (2-aromatic vinyl)-1-*N*-methylquinolinium derivatives, the product was obtained as a green-yellow solid. Mp > 200 °C. ^{1}H NMR (400 Hz, DMSO-d_6): δ 8.28 (d, 1H, J = 12.0), 8.13 (d, 1H, J = 8.0), 8.02 (t, 1H, J = 8.0), 7.88 (t, 1H, J = 16.0), 7.73 (t, 1H, J = 8.0), 7.59 (d, 1H, J = 16.0), 7.48 (d, 2H, J = 4.0), 7.42 (d, 1H, J = 8.0), 6.95 (d, 1H, J = 8.0), 4.23 (s, 3H), 3.91 (s, 3H), 3.77 (s, 4H), 3.73 (s, 4H), 3.07 (s, 4H), 2.63 (s, 4H), 2.30 (s, 3H). ^{13}C NMR (100 MHz, DMSO-d_6) δ 159.3, 154.2, 151.7, 143.5, 140.8, 136.6, 133.7, 129.2, 126.5, 126.2, 123.2, 119.7, 119.2, 117.5, 117.3, 111.2, 105.0, 66.2, 55.8, 54.2, 51.5, 50.2, 45.4, 38.2. Purity: 99.0% by HPLC. ESI-HRMS ($C_{28}H_{35}N_4O_2$): calcd, 459.2755 [M]$^+$; found, 459.2746.

(*E*)-1-Methyl-4-(4-methylpiperazin-1-yl)-2-(4-morpholinostyryl)quinolin -1-ium Iodide (22). Following general procedure B for (2-aromatic vinyl)-1-*N*-methylquinolinium derivatives, the product was obtained as a green-yellow solid. Mp > 200 °C. ^{1}H NMR (400 Hz, DMSO-d_6): δ 8.27 (d, 1H, J = 8.0), 8.12 (d, 1H, J = 8.0), 8.01−7.95 (t, 1H, J = 8.0), 7.88 (d, 1H, J = 12.0), 7.79 (d, 2H, J = 12.0), 7.72 (t, 1H, J = 8.0), 7.48 (t, 2H, J = 8.0),7.05 (d, 2H, J = 8.0), 4.22 (s, 3H), 3.75 (s, 8H), 3.32 (s, 4H), 2.63 (s, 4H), 2.31 (s, 3H). ^{13}C NMR (100 MHz, DMSO-d_6): δ 159.0, 154.4, 152.4, 143.7, 140.7, 133.5, 130.3, 126.3, 126.0, 125.1, 119.6, 119.1, 115.0, 113.9, 104.7, 65.8, 54.2, 51.5, 47.0, 45.5, 38.1. Purity: 96.6% by HPLC. ESI-HRMS ($C_{27}H_{33}N_4O$): calcd, 429.2649 [M]$^+$; found, 429.2649.

(*E*)-2-(2-(1*H*-Indol-2-yl)vinyl)-1-methyl-4-(4-methylpiperazin-1-yl)quinolin 1-ium Iodide (23). Following general procedure B for (2-aromatic vinyl)-1-*N*-methylquinolinium derivatives, the product was obtained as a green-yellow solid. Mp > 200 °C. ^{1}H NMR (400 Hz, DMSO-d_6): δ 12.01 (s, 1H), 8.27 (t, 2H, J = 8.0), 8.17 (s, 2H), 8.12 (d, 1H, J = 8.0), 8.00 (t,1H, J = 8.0), 7.72 (t, 1H, J = 8.0), 7.53 (s, 2H), 7.41 (d, 1H, J = 16.0), 7.28 (d, 2H, J = 4.0), 4.25 (s, 3H), 3.72(s, 4H), 2.65 (s, 4H), 2.32 (s, 3H). ^{13}C NMR (100 MHz, DMSO-d_6): δ 158.8, 155.2, 140.7, 138.8, 137.4, 133.4, 132.5, 126.3, 126.0, 125.0, 122.9, 121.2, 120.2, 119.8, 119.1, 113.6, 112.6, 104.3, 54.2, 51.5, 48.5, 45.5, 37.9. Purity: 97.8% by HPLC. ESI-HRMS ($C_{25}H_{27}N_4$): calcd, 383.2230 [M]$^+$; found, 383.2212.

(*E*)-2-(2-(9-Ethyl-9*H*-carbazol-3-yl)vinyl)-1-methyl-4-(4-methyl piperazin-1-yl)quinolin-1-ium Iodide (24). Following general procedure B for (2-aromatic vinyl)-1-*N*-methylquinolinium derivatives, the product was obtained as a green-yellow solid. Mp > 200 °C. ^{1}H NMR (400 Hz, DMSO-d_6): δ 8.73 (s, 1H), 8.31 (d, 1H, J = 12.0), 8.23 (d, 1H, J = 8.0), 8.16 (d, 1H, J = 8.0), 8.13 (s, 1H), 8.07−8.01 (m, 2H, J = 8.0, J = 8.0), 7.75 (t, 3H, J = 8.0), 7.69 (d, 1H, J = 8.0), 7.57−7.51 (m, 2H, J = 8.0, J = 8.0), 7.30 (t, 1H, J = 8.0), 4.53−4.48 (m, 2H, J = 4.0, J = 8.0), 4.29 (s, 3H), 3.78 (s, 4H), 2.65 (s, 4H), 2.32 (s, 3H), 1.36 (t, 3H, J = 8.0). ^{13}C NMR (100 MHz, DMSO-d_6) δ 159.1, 154.2, 144.8, 140.8, 140.6, 140.0, 133.4, 126.7, 126.3, 126.2, 126.1, 126.0, 122.5, 122.1, 121.7, 120.5, 119.6, 119.0, 116.1, 109.6, 109.5, 104.8, 54.2, 51.6, 45.5, 38.2, 37.2, 13.8. Purity: 98.6% by HPLC. ESI-HRMS ($C_{31}H_{33}N_4$): calcd, 461.2700 [M]$^+$; found, 461.2703.

(*E*)-2-(2-(9-Ethyl-9*H*-carbazol-3-yl)vinyl)-4-(4-(2-hydroxyethyl)piperazin-1-yl)-1-methylquinolin-1-ium Iodide (25). Following general procedure B for (2-aromatic vinyl)-1-*N*-methylquinolinium derivatives, the product was obtained as a green-yellow solid. Mp > 200 °C. ^{1}H NMR (400 Hz, DMSO-d_6): δ 8.73 (s, 1H), 8.31 (d, 1H, J = 8.0), 8.23 (d, 1H, J = 8.0), 8.13 (t, 2H, J = 8.0), 8.07−8.00 (m, 2H), 7.76−7.72 (m, 3H), 7.68 (d, 1H, J = 8.0), 7.56−7.51(m, 2H), 7.30 (t, 1H, J = 8.0), 4.51(t, 2H, J = 4.0), 4.29 (s, 3H), 3.80 (s, 4H), 3.60 (t, 2H, J = 8.0, J = 4.0), 2.76 (s, 4H), 2.55 (t, 2H, J = 8.0), 1.36 (t, 3H, J = 8.0). ^{13}C NMR (100 MHz, DMSO-d_6): δ 159.0, 154.2, 144.7, 140.8, 140.6, 140.1, 133.5, 126.7, 126.4, 126.3, 126.2, 126.0, 122.6, 122.2, 121.7, 120.6, 119.6, 119.5, 119.0, 116.1, 109.6, 109.5, 104.7, 59.8, 58.5, 52.8, 51.7, 38.2 37.2, 13.8. Purity: 96.7% by HPLC. ESI-HRMS ($C_{32}H_{35}N_4O$): calcd, 491.2805 [M]$^+$; found, 491.2778.

(*E*)-4-(4-(2-(Dimethylamino)ethyl)piperazin-1-yl)-2-(2-(9-ethyl-9*H*-carbazol-3 -yl)vinyl)-1-methylquinolin-1-ium Iodide (26). Following general procedure B for (2-aromatic vinyl)-1-*N*-methylquinolinium derivatives, the product was obtained as a green-yellow solid. Mp > 200 °C. ^{1}H NMR (400 Hz, DMSO-d_6): δ 8.75 (s, 1H), 8.32 (d, 1H, J = 8.0), 8.23 (d, 1H, J = 8.0), 8.16 (t, 2H, J = 8.0), 8.07 (d, 1H, J = 12.0), 8. 01 (t, 1H, J = 8.0), 7.81−7.73 (m, 3H), 7.70 (d, 1H, J = 8.0),7.59 (s, 1H), 7.57−7.52 (m, 1H, J = 4.0, J = 8.0), 7.31 (t, 1H, J = 8.0), 4.55−4.50 (m, 2H, J = 8.0, J = 8.0), 4.31 (s, 3H), 3.82 (s, 4H), 3.32 (s, 2H), 3.15 (t, 2H, J = 4.0), 2.83 (s, 6H), 2.73 (s, 4H), 1.88 (s, 2H), 1.36 (t, 3H, J = 8.0). ^{13}C NMR (100 MHz, DMSO-d_6): δ 159.1, 154.4, 144.9, 141.0, 140.8, 140.1, 133.6, 126.7, 126.4, 126.2, 126.1, 122.6, 122.2, 121.7, 120.8, 120.5, 120.1, 119.7, 119.6, 119.2, 116.3, 109.9, 109.7, 109.6, 109.6, 104.9, 55.5, 54.2, 52.2, 51.6, 42.4, 38.2, 37.2, 20.9, 13.8. Purity: 99.7% by HPLC. ESI-HRMS ($C_{34}H_{40}N_5$): calcd, 518.3278 [M]$^+$; found, 518.3160.

(*E*)-4-(4-(3-Dimethylamino)propyl)piperazin-1-yl)-2-(2-(9-ethyl-9*H*-carbazol-3-yl) vinyl)-1-methylquinolin-1-ium Iodide

DOI: 10.1021/acs.jmedchem.5b00139
J. Med. Chem. XXXX, XXX, XXX−XXX

(27). Following general procedure B for (2-aromatic vinyl)-1-*N*-methylquinolinium derivatives, the product was obtained as a green-yellow solid. Mp > 200 °C. ^{1}H NMR (400 Hz, DMSO-d_6): δ 8.75 (s, 1H), 8.34 (d, 1H, J = 12.0), 8.23 (d, 1H, J = 8.0), 8.16 (t, 2H, J = 8.0), 7.76 (t, 3H, J = 8.0), 7.70 (d, 1H, J = 8.0), 7.60 (s, 1H), 7.54 (t, 1H, J = 8.0),7.31 (t, 1H, J = 8.0), 4.55−4.49 (m, 2H, J = 8.0, J = 8.0), 4.31 (s, 3H), 3.84 (s, 4H), 3.31 (s, 4H), 2.86 (s, 6H), 2.80 (s, 4H), 1.36 (t, 3H, J = 8.0). ^{13}C NMR (100 MHz, DMSO-d_6): δ 159.1, 154.4, 144.9, 141.0, 140.8, 140.1, 133.6, 126.7, 126.4, 126.2, 126.1, 122.6, 122.2, 121.7, 120.8, 120.5, 120.1, 119.7, 119.6, 119.2, 116.3, 109.9, 109.7, 109.6, 109.6, 104.9, 55.5, 54.2, 52.2, 51.6, 42.4, 38.2, 37.24, 20.9, 13.8. Purity: 98.3% by HPLC. ESI-HRMS ($C_{35}H_{42}N_5$): calcd, 532.3435 $[M]^+$; found, 532.3314.

(*E*)-2-(2-(9-Ethyl-9*H*-carbazol-3-yl)vinyl)-1-methyl-4-(piperidin-1-yl)quinolin-1-ium Iodide (28). Following general procedure B for (2-aromatic vinyl)-1-*N*-methylquinolinium derivatives, the product was obtained as a green-yellow solid. Mp > 200 °C. ^{1}H NMR (400 Hz, DMSO-d_6): δ 8.72 (s, 1H), 8.29 (d, 1H, J = 12.0), 8.23 (d, 1H, J = 8.0), 8.13 (s, 1H), 8.12−8.02 (m, 4H), 7.77−7.67 (m, 3H), 7.52 (t, 2H, J = 12.0, J = 4.0), 7.30 (t, 1H, J = 8.0), 4.50 (s, 2H), 4.27 (s, 3H), 3.76 (s, 4H), 1.85 (s, 4H), 1.79 (s, 2H), 1.36 (t, 3H, J = 8.0). ^{13}C NMR (100 MHz, DMSO-d_6): δ 159.5, 154.2, 144.4, 140.9, 140.8, 140.1, 133.5, 126.6, 126.5, 126.4, 126.2, 125.9, 122.6, 122.2, 121.6, 120.5, 119.7, 119.6, 119.1, 116.4, 109.7, 109.6, 104.4, 52.8, 38.0, 37.2, 25.4, 23.5, 13.7. Purity: 99.1% by HPLC. ESI-HRMS ($C_{31}H_{32}N_3$): calcd, 446.2591 $[M]^+$; found, 446.2555.

(*E*)-2-[(9-Ethyl-9*H*-carbazol-3-yl)ethenyl]quinoline (29). A suspension of 2-methylquinoline (1.0 mmol), 9-ethyl-9*H*-carbazol-3-aldehyde (1.05 mmol), and acetic anhydride (15 mL) was heated at 125 °C for 24 h. After completion of the reaction, the reaction mixture was allowed to cool to room temperature and then poured into ice−water (40 mL), and then aqueous NaOH was added to make the solution basic. The solids formed were filtered off and washed with water, and the crude product was purified by using flash column chromatography with CH_2Cl_2/petroleum ether (3:2) elution to give desired product **29** as a pale yellow solid in 67% yield. Mp 183.5−184.9 °C. ^{1}H NMR (400 MHz, $CDCl_3$): δ 8.37 (d, J = 4.0 Hz, 1H), 8.12 (d, J = 4.0 Hz, 3H), 7.95−7.86 (m, 1H), 7.81−7.71 (m, 4H), 7.49−7.41 (m, 5H), 7.26 (t, J = 4.0 Hz, 1H), 4.44−4.31 (m, 2H), 1.48−1.44 (m, 3H). ^{13}C NMR (100 MHz, $CDCl_3$): δ 156.7, 148.3, 140.4, 140.4, 136.2, 135.6, 129.6, 129.1, 127.7, 127.5, 127.2, 126.3, 126.0, 125.8, 125.2, 123.4, 123.0, 120.5, 119.9, 119.3, 119.1, 108.8, 108.7, 37.7, 13.9. Purity: 99.1% by HPLC. ESI-HRMS ($C_{25}H_{20}N_2$): cacld, 349.1699 $[M + H]^+$; found, 349.1709.

General Procedure C: Preparation of Compounds 30−32. A suspension of compound **6a** or **6b** (1.0 mmol), various aromatic aldehydes (1.05 mmol), and acetic anhydride (15 mL) was heated at 150 °C for 36 h. After completion of the reaction, the reaction mixture was allowed to cool to room temperature and poured into ice−water (40 mL), and then aqueous NaOH was added to make the solution basic. The solids formed were filtered and washed with water, and the crude product was purified by using flash column chromatography with CH_2Cl_2/petroleum ether (1:1) or EtOAc/methanol (200:3) elution to give the desired products.

(*E*)-4-(4-Methylpiperazin-1-yl)-2-(4-(morpholin-1-yl)styryl)-quinoline (30). Compound **6a** was reacted with 4-morpholinylbenzaldehyde following general procedure C to give the desired product **30** as an orange solid in 66% yield. Mp 206.6−208.9 °C. ^{1}H NMR (400 MHz, $CDCl_3$): δ 7.99 (d, J = 8.9 Hz, 2H), 7.65−7.45 (m, 4H), 7.44−7.34 (m, 1H), 7.21 (d, J = 12.0 Hz, 1H), 7.14−7.00 (m, 1H), 6.92 (s, 2H), 3.87 (s, 4H), 3.25 (s, 8H), 2.74 (s, 4H), 2.51−2.33 (m, 3H). ^{13}C NMR (100 MHz, $CDCl_3$): δ 157.0, 156.8, 151.3, 149.6, 133.8, 129.6, 129.2, 128.4, 128.1, 126.5, 124.7, 123.4, 122.6, 115.2, 106.8, 66.8, 55.2, 52.1, 48.6, 46.1. Purity: 98.6% by HPLC. ESI-HRMS ($C_{26}H_{30}N_4O$): cacld, 415.2492 $[M + H]^+$; found, 415.2474.

(*E*)-4-(4-Methylpiperazin-1-yl)-2-[(9-ethyl-9*H*-carbazol-3-yl)-ethenyl]quinoline (31). Compound **6a** was reacted with 9-ethyl-9*H*-carbazol-3-aldehyde according to general procedure C to give the desired product **31** as a yellow solid in 66% yield. Mp 188.2−191.3 °C. ^{1}H NMR (400 MHz, $CDCl_3$): δ 8.38 (s, 1H), 8.13 (d, J = 8.0 Hz, 1H), 8.06 (d, J = 8.0 Hz, 1H), 7.98 (d, J = 8.0 Hz, 1H), 7.87 (d, J = 16 Hz, 1H), 7.81 (d, J = 8.0 Hz, 1H), 7.64 (t, J = 8.0 Hz, 1H), 7.50−7.38 (m, 5H), 7.28 (d, J = 8.0 Hz, 1H), 7.18 (s, 1H), 4.40−4.37 (m, 2H), 3.35 (s, 4H), 2.77 (s, 4H), 2.46 (s, 3H), 1.46 (t, J = 8.0 Hz, 3H). ^{13}C NMR (100 MHz, $CDCl_3$): δ 157.0, 157.0, 149.7, 140.4, 140.3, 135.1, 129.7, 129.2, 127.8, 126.7, 126.0, 125.1, 124.7, 123.5, 123.4, 123.0, 122.7, 120.5, 119.8, 119.2, 108.8, 108.7, 106.8, 55.2, 52.1, 46.2, 37.7, 13.9. Purity: 99.9% by HPLC. ESI-HRMS($C_{30}H_{30}N_4$): calcd, 447.2543 $[M + H]^+$; found, 447.2521.

(*E*)-4-(Piperid-1-yl)-2-[(9-ethyl-9*H*-carbazol-3-yl)ethenyl]-quinoline (32). Compound **6b** was reacted with 9-ethyl-9*H*-carbazol-3-aldehyde following general procedure C to give the desired product **32** as an orange-yellow solid in 65% yield. Mp 185.9−187.4 °C. ^{1}H NMR (400 MHz, $CDCl_3$): δ 8.37 (d, J = 6.0 Hz, 1H), 8.12 (t, J = 8.0 Hz, 1H), 8.06 (s, 1H), 7.97 (t, J = 8.0 Hz, 1H), 7.88−7.76 (m, 2H), 7.64−7.60 (m, 1H), 7.49−7.41 (m, 5H), 7.27−7.24 (m, 1H), 7.16 (d, J = 8.0 Hz, 1H), 4.40−4.35 (m, 2H), 3.26 (s, 4H), 1.88 (s, 4H), 1.73 (s, 2H), 1.48−1.40 (m, 3H). ^{13}C NMR (100 MHz, $CDCl_3$): δ 158.3, 156.9, 140.4, 140.3, 129.3, 128.9, 127.8, 127.5, 125.9, 125.1, 124.5, 123.8, 123.4, 123.0, 122.9, 121.8, 121.4, 119.8, 119.2, 108.8, 108.7, 108.0, 106.3, 53.7, 37.7, 26.2, 24.5, 13.9. Purity: 98.9% by HPLC. ESI-HRMS($C_{30}H_{29}N_3$): calcd, 432.2434 $[M + H]^+$; found, 432.2421.

Oligonucleotides. The RNA oligonucleotides used were the following: A10-RNA-Wt, 5′-UGGGGGACGGGUAGGGGCGGGAG-GUAGGGG-3′; A10-RNA-Mut, 5′-UAGAAGACGA-AUAGAAGCGAAAAGUAGAAG-3′. The 5′-end biotinylated A10-RNA-Wt and 5′-end biotinylated A10-RNA-Mut sequences were purchased from Integrated DNA Technologies, Inc. The A10-RNA-Wt sequence, 5′-end labeled with Cy3 and 3′-end labeled with Cy5, was also purchased from Integrated DNA Technologies, Inc. The DNA oligonucleotide used was the DNA antisense oligonucleotide (AS), 5′-CCCCTACCTCCCGCCCCTACCCGTCCCCCA-3′. The AS DNA sequence was purchased from Life Technologies, Inc.

Surface Plasmon Resonance (SPR). SPR was performed on a ProteOn XPR36 protein interaction system (Bio-Rad Laboratories, Hercules, CA) using a neutravidin-coated GLH sensor chip. The 5′-end biotinylated RNAs (A10-RNA-Wt or A10-RNA-Mut) were immobilized on the sensor chip in degassed SPR running buffer (50 mM Tris-HCl, pH 7.5, 100 mM KCl). For the initial screening experiment, the ligands were diluted with running buffer to the same concentration (10 μM). In the RNA binding experiments, solutions of ligands **1**−**32** were freshly prepared in running buffer by serial dilutions from stock solution. For both experiments, the ligand was injected at a flow rate of 20 μL/min during the association phase, which was followed by a disassociation phase. The GLH sensor chip was regenerated using a brief injection of 50 mM NaOH between consecutive measurements. The equilibrium dissociation constants (K_D) were determined with ProteOnmanager software using the equilibrium method.

Native Gel Electrophoresis Assay. The A10-RNA-Wt sequence labeled with Cy3 and Cy5 was folded in the presence of 100 mM KCl, 10 mM Tris-HCl, and 0.1 mM EDTA (pH 7.5) by heating for 5 min at 95 °C followed by cooling to room temperature over a 90 min period. After cooling, the RNA samples (2 μM) were incubated with various concentrations of the DNA antisense oligonucleotide (AS) or compound **24** for 15 and 5 min, respectively, at room temperature in the dark. The samples were then loaded on a native 16% gel and electrophoresed at 4 °C before being exposed to a gel image system (Tanon-4500 sf).

cDNA Constructs. Plasmids A10-Wt, A10-Mut, 5′UTR-Wt, and 5′UTR-Mut were constructed as previously described.[21] Briefly, the ADAM10 G-quadruplex motif, the 5′-UTR of ADAM10, and their QGRS motif-mutated variants (Figure 2B) inserted in front of the *Renilla luciferase* of the psiCHECK-2 vector (Promega) were generated by PCR using the unique Nhe I restriction site upstream from the *Renilla luciferase* start codon. All cDNAs were verified by sequencing.

Cell Culture. HeLa cells were cultured in Dulbecco's modified Eagle medium (DMEM) supplemented with 10% fetal bovine serum and 2 mM glutamine. The HEK-APP cell line was cultured in DMEM

DOI: 10.1021/acs.jmedchem.5b00139
J. Med. Chem. XXXX, XXX, XXX−XXX

supplemented with 10% fetal bovine serum, 2 mM glutamine, and 0.2 mg/mL G418.

Dual Luciferase Reporter Assay. HeLa cells were transfected with 0.8 μg of A10-Wt, A10-Mut, or A10-Del plasmid using LipofectAMINE 2000 (Invitrogen) as a transfecting reagent. Transfections were performed by addition of the vector (250 ng/well). The culture medium was replaced 12 h after transfection, and the cells were transiently transfected with either the AS or a random deoxyoligonucleotide, each at a final concentration of 200 nM. After treatment for 24 h, cell lysates were prepared, and the luciferase activity was measured with the dual-luciferase reporter assay system (Promega) according to the manufacturer's instructions. In experiments for 11 selected compounds, after transfection with A10-Wt, A10-Mut, or A10-Del plasmid as above, the cells were transiently incubated with a single concentration of selected compounds (2 μM). After treatment for 24 h, the luciferase activity was measured with the dual-luciferase reporter assay system. In further experiments for the most potent compound, **24**, after transfection with 0.8 μg of A10-Wt, A10-Mut, A10-Del, 5′UTR-Wt, or 5′UTR-Mut plasmid for 12 h, the HeLa cells were incubated with 0, 0.5, 1, or 2.5 μM **24** for 24 h, and the dual-luciferase reporter assays were performed. The quantification was performed using a multimode reader (Molecular Devices). The *Renilla* luciferase activity was normalized to the firefly luciferase activity. All of the above samples were also prepared for RT-PCR assay.

Protein Analysis. HEK-APP cells were plated in 10 cm dishes, and 48 h after treatment with 0, 0.5, 0.75, 1, or 1.5 μM **24**, cell lysates were prepared using lysis buffer containing 50 mM Tris-HCl, pH 7.6, 150 mM NaCl, 2 mM EDTA, 1% Triton X-100, and protease inhibitors (Sigma) and analyzed for ADAM10, APP, and β-actin protein levels by immunoblotting. The cell lysates were collected, transferred to Eppendorf tubes, and centrifuged at 15 000*g* for 2 min to collect the cell debris. For analysis of APP processing, equal amounts of the conditioned cell culture medium were collected and analyzed for sAPPα and $A\beta_{40}$ protein level by immunoblotting and ELISA, respectively. All of the above samples were also prepared for analysis by RT-PCR.

Western Blotting. Protein samples denatured in SDS sample buffer (125 mmol/L Tris-HCl, pH 7.0, 50% (v/v) glycerol, 2% (w/v) SDS, 5% (v/v) mercaptoethanol, and 0.01% (w/v) bromophenol blue) were subjected to SDS−PAGE and blotted onto polyvinylidene difluoride (Millipore) membranes. The blotted membranes were blocked with 5% (w/v) skim milk in Tris-buffered saline containing 0.1% (v/v) Tween 20 for 1 h and then incubated with primary antibodies for 16 h at 4 °C. After three washes in Tris-buffered saline containing 0.1% (v/v) Tween 20, the membranes were incubated with anti-mouse or anti-rabbit peroxidase-linked secondary antibody (1:2000; Santa Cruz) for 2 h. The immunoreactive signals were detected using a ChemiDoc XRS imaging system (Bio Rad) and quantified with Image Lab 3.0 software (Bio Rad). Key proteins were examined by Western blotting using specific antibodies including anti-ADAM10 (1:1000; Abcam), anti-APP (1:1000; Convance), anti-sAPPα (1:1000; Convance), and anti-β-actin (1:1000; Cell Signaling). Immunolabeled bands were quantified by densitometry using Quantity ONE software (Bio Rad), and representative blots are shown. The ADAM10 and APP levels were normalized to the β-actin levels where indicated.

Enzyme-Linked Immunosorbent Assay (ELISA). HEK-APP cell culture media were collected to quantify the secreted $A\beta_{40}$ peptide by sandwich immunoassay using an ELISA kit (Invitrogen) according to the manufacturer's instructions.

Reverse-Transcription PCR (RT-PCR). Total RNA was isolated from HeLa cells or HEK-APP cells samples using RNAiso Plus (Takara) according to the manufacturer's protocol. After the first strand cDNA was synthesized using Oligo (dT), the cDNA was used for amplification of specific target genes by PCR. β-Actin was used as the RNA loading control. The PCR products were separated on 1.5% (w/v) agarose gels and analyzed using the AlphaImager EC Imaging System (Alpha Innotech). The PCR primer sequences were as follows. β-Actin: sense, 5′-CTGAATCTGCACCAAGCATGA-3′, antisense, 5′-TAAAACGCAGCTCAGTAACAGTCC-3′. *Renilla luciferase*: sense, 5′-TCTTTGTGGGCCACGACTGGGG-3′, antisense, 5′-GGCAGCGAACTCCTCAGGCTCC-3′. Firefly luciferase: sense, 5′-GCCGTGGCCAAGCGCTTTCATC-3′, antisense, 5′-CTCCCAGGGTCTTGCCGGTGTC-3′. ADAM10: sense, 5′-TTTGATGATGGCGTACTTGG-3′, antisense, 5′-AGTTTGTC-CCCAGATGTTGC-3′. APP: sense, 5′-CACCACAGAG-TCTGTGGAAGA-3′, antisense, 5′-AGGTGTCTGAGATACTTGT-3′. For each corresponding RNA sample used in the dual-luciferase reporter assay, the *Renilla* luciferase RNA expression was normalized to firefly luciferase as described.[21] The ADAM10 and APP levels were normalized to β-actin levels where indicated. The quantification was performed by densitometry using Quantity ONE software (Bio Rad).

Measurement of ADAM10 Activity. α-Secretase (ADAM10) activity was determined using recombinant human ADAM10 protein (R&D) and a fluorogenic α-secretase substrate (MERCK). Before performance of the activity assay, the ADAM10 protein was incubated with various concentrations of **24** (0, 0.25, 0.5, 1, 2, 4 μM) for 20 min. A total of 50 μL of sample (total protein 50 ng) was added to each well followed by 50 μL of 2× reaction buffer (50 μM Tris, 4 μM $ZnCl_2$, 0.01% (w/v) Brij-35, pH 9.0) and 20 μM α-secretase substrate. The samples were then incubated in the dark at 37 °C for 1 h. The fluorescence was read at excitation and emission wavelengths of 340 and 490 nm, respectively, using a monochromator-based multimode microplate reader (M1000, Tecan). α-Secretase activity is proportional to the fluorimetric reaction and is expressed as nmol/mg protein per minute.

■ ASSOCIATED CONTENT

Supporting Information

Additional experiment results, ^1H and ^{13}C NMR spectra, and LC/MS and HPLC assay data for compounds. This material is available free of charge via the Internet at http://pubs.acs.org.

■ AUTHOR INFORMATION

Corresponding Author

*Phone: 8620-39943056. Fax: 8620-39943056. E-mail: ceshzs@mail.sysu.edu.cn.

Author Contributions

‡J.D. and Z.-Q.L. contributed equally.

Notes

The authors declare no competing financial interest.

■ ACKNOWLEDGMENTS

We thank the Natural Science Foundation of China (Grants 81273433, 91213302, and 81330077), Specialized Research Fund for the Doctoral Program of Higher Education of China (Grant 20110171110051), and Guangdong Provincial Key Laboratory of Construction Foundation (Grant 2011A060901014) for financial support of this study.

■ ABBREVIATIONS USED

ADAM10, a disintegrin and metalloprotease 10; Aβ, β-amyloid; AD, Alzheimer's disease; QGRS, G-quadruplex forming G-rich sequence; UTR, untranslated region; SPR, surface plasmon resonance; HEK-APP, HEK 293 cell line stably overexpressing Swedish-mutated amyloid precursor protein; APP, amyloid precursor protein; ADAM, a family of disintegrin and metalloproteinases; PKC, protein kinase C; GABA-A, γ-aminobutyric acid type A; PDE4, phosphodiesterase 4; MTT, methylthiazolyltetrazolium; MST, microscale thermophoresis; sAPPα, human soluble amyloid precursor protein α; AS, DNA antisense oligonucleotide; RT-PCR, reverse transcription PCR; RU, relative intensity; SAR, struture−activity relationship; *p*-TSA, *p*-toluenesulfonic acid; FMRP, fragile-X mental retardation protein; hnRNP, heterogeneous nuclear ribonucleopro-

DOI: 10.1021/acs.jmedchem.5b00139
J. Med. Chem. XXXX, XXX, XXX−XXX

tein; ASF/SF2, alternative splicing factor/splicing factor 2; MS, mass spectra; HRMS, high-resolution mass spectra; Mp, melting point; EDTA, ethylenediaminetetraacetic acid; DMEM, Dulbecco's modified Eagle medium; FBS, fetal bovine serum; SDS, sodium dodecyl sulfate; ELISA, enzyme-linked immunosorbent assay

REFERENCES

(1) Hardy, J.; Selkoe, D. J. The amyloid hypothesis of Alzheimer's disease: progress and problems on the road to therapeutics. *Science* **2002**, *297*, 353−356.

(2) Haass, C.; Selkoe, D. J. Soluble protein oligomers in neurodegeneration: lessons from the Alzheimer's amyloid beta-peptide. *Nat. Rev. Mol. Cell Biol.* **2007**, *8*, 101−112.

(3) Meziane, H.; Dodart, J. C.; Mathis, C.; Little, S.; Clemens, J.; Paul, S. M.; Ungerer, A. Memory-enhancing effects of secreted forms of the beta-amyloid precursor protein in normal and amnestic mice. *Proc. Natl. Acad. Sci. U.S.A.* **1998**, *95*, 12683−12688.

(4) Furukawa, K.; Sopher, B. L.; Rydel, R. E.; Begley, J. G.; Pham, D. G.; Martin, G. M.; Fox, M.; Mattson, M. P. Increased activity-regulating and neuroprotective efficacy of alpha-secretase-derived secreted amyloid precursor protein conferred by a C-terminal heparin-binding domain. *J. Neurochem.* **1996**, *67*, 1882−1896.

(5) Fahrenholz, F. Alpha-secretase as a therapeutic target. *Curr. Alzheimer Res.* **2007**, *4*, 412−417.

(6) Koike, H.; Tomioka, S.; Sorimachi, H.; Saido, T. C.; Maruyama, K.; Okuyama, A.; Fujisawa-Sehara, A.; Ohno, S.; Suzuki, K.; Ishiura, S. Membrane-anchored metalloprotease MDC9 has an alpha-secretase activity responsible for processing the amyloid precursor protein. *Biochem. J.* **1999**, *343*, 371−375.

(7) Buxbaum, J. D.; Liu, K. N.; Luo, Y.; Slack, J. L.; Stocking, K. L.; Peschon, J. J.; Johnson, R. S.; Castner, B. J.; Cerretti, D. P.; Black, R. A. Evidence that tumor necrosis factor alpha converting enzyme is involved in regulated alpha-secretase cleavage of the Alzheimer amyloid protein precursor. *J. Biol. Chem.* **1998**, *273*, 27765−27767.

(8) Lammich, S.; Kojro, E.; Postina, R.; Gilbert, S.; Pfeiffer, R.; Jasionowski, M.; Haass, C.; Fahrenholz, F. Constitutive and regulated alpha-secretase cleavage of Alzheimer's amyloid precursor protein by a disintegrin metalloprotease. *Proc. Natl. Acad. Sci. U.S.A.* **1999**, *96*, 3922−3927.

(9) Lichtenthaler, S. F. alpha-secretase in Alzheimer's disease: molecular identity, regulation and therapeutic potential. *J. Neurochem.* **2010**, *116*, 10−21.

(10) Postina, R.; Schroeder, A.; Dewachter, I.; Bohl, J.; Schmitt, U.; Kojro, E.; Prinzen, C.; Endres, K.; Hiemke, C.; Blessing, M.; Flamez, P.; Dequenne, A.; Godaux, E.; van Leuven, F.; Fahrenholz, F. A disintegrin-metalloproteinase prevents amyloid plaque formation and hippocampal defects in an Alzheimer disease mouse model. *J. Clin. Invest.* **2004**, *113*, 1456−1464.

(11) Kim, M.; Suh, J.; Romano, D.; Truong, M. H.; Mullin, K.; Hooli, B.; Norton, D.; Tesco, G.; Elliott, K.; Wagner, S. L.; Moir, R. D.; Becker, K. D.; Tanzi, R. E. Potential late-onset Alzheimer's disease-associated mutations in the ADAM10 gene attenuate alpha-secretase activity. *Hum. Mol. Genet.* **2009**, *18*, 3987−3996.

(12) Marcinkiewicz, M.; Seidah, N. G. Coordinated expression of beta-amyloid precursor protein and the putative beta-secretase BACE and alpha-secretase ADAM10 in mouse and human brain. *J. Neurochem.* **2000**, *75*, 2133−2143.

(13) Colciaghi, F.; Borroni, B.; Pastorino, L.; Marcello, E.; Zimmermann, M.; Cattabeni, F.; Padovani, A.; Di Luca, M. alpha-Secretase ADAM10 as well as alpha-APPs is reduced in platelets and CSF of Alzheimer disease patients. *Mol. Med.* **2002**, *8*, 67−74.

(14) Tippmann, F.; Hundt, J.; Schneider, A.; Endres, K.; Fahrenholz, F. Up-regulation of the alpha-secretase ADAM10 by retinoic acid receptors and acitretin. *FASEB J.* **2009**, *23*, 1643−54.

(15) Hartmann, D.; de Strooper, B.; Serneels, L.; Craessaerts, K.; Herreman, A.; Annaert, W.; Umans, L.; Lubke, T.; Lena Illert, A.; von Figura, K.; Saftig, P. The disintegrin/metalloprotease ADAM 10 is essential for Notch signalling but not for alpha-secretase activity in fibroblasts. *Hum. Mol. Genet.* **2002**, *11*, 2615−24.

(16) Jorissen, E.; Prox, J.; Bernreuther, C.; Weber, S.; Schwanbeck, R.; Serneels, L.; Snellinx, A.; Craessaerts, K.; Thathiah, A.; Tesseur, I.; Bartsch, U.; Weskamp, G.; Blobel, C. P.; Glatzel, M.; De Strooper, B.; Saftig, P. The disintegrin/metalloproteinase ADAM10 is essential for the establishment of the brain cortex. *J. Neurosci.* **2010**, *30*, 4833−44.

(17) De Strooper, B.; Vassar, R.; Golde, T. The secretases: enzymes with therapeutic potential in Alzheimer disease. *Nat. Rev. Neurol.* **2010**, *6*, 99−107.

(18) Desire, L.; Marcade, M.; Peillon, H. Clinical trials of EHT 0202, a neuroprotective and procognitive alpha-secretase stimulator for Alzheimer's disease. *Alzheimer's Dementia* **2009**, *5* (Supp.), 255−256.

(19) Marcade, M.; Bourdin, J.; Loiseau, N.; Peillon, H.; Rayer, A.; Drouin, D.; Schweighoffer, F.; Desire, L. Etazolate, a neuroprotective drug linking GABA(A) receptor pharmacology to amyloid precursor protein processing. *J. Neurochem.* **2008**, *106*, 392−404.

(20) Donmez, G.; Wang, D.; Cohen, D. E.; Guarente, L. SIRT1 suppresses beta-amyloid production by activating the alpha-secretase gene ADAM10. *Cell* **2010**, *142*, 320−332.

(21) Lammich, S.; Buell, D.; Zilow, S.; Ludwig, A. K.; Nuscher, B.; Lichtenthaler, S. F.; Prinzen, C.; Fahrenholz, F.; Haass, C. Expression of the anti-amyloidogenic secretase ADAM10 is suppressed by its 5′-untranslated region. *J. Biol. Chem.* **2010**, *285*, 15753−15760.

(22) Lammich, S.; Kamp, F.; Wagner, J.; Nuscher, B.; Zilow, S.; Ludwig, A. K.; Willem, M.; Haass, C. Translational repression of the disintegrin and metalloprotease ADAM10 by a stable G-quadruplex secondary structure in its 5′-untranslated region. *J. Biol. Chem.* **2011**, *286*, 45063−45072.

(23) Endres, K.; Fahrenholz, F. Regulation of alpha-secretase ADAM10 expression and activity. *Exp. Brain Res.* **2011**, *217*, 343−352.

(24) Millevoi, S.; Moine, H.; Vagner, S. G-quadruplexes in RNA biology. *Wiley Interdiscip. Rev. RNA* **2012**, *3*, 495−507.

(25) Murat, P.; Zhong, J.; Lekieffre, L.; Cowieson, N. P.; Clancy, J. L.; Preiss, T.; Balasubramanian, S.; Khanna, R.; Tellam, J. G-quadruplexes regulate Epstein−Barr virus-encoded nuclear antigen 1 mRNA translation. *Nat. Chem. Biol.* **2014**, *10*, 358−364.

(26) Kumari, S.; Bugaut, A.; Huppert, J. L.; Balasubramanian, S. An RNA G-quadruplex in the 5′ UTR of the NRAS proto-oncogene modulates translation. *Nat. Chem. Biol.* **2007**, *3*, 218−221.

(27) Arora, A.; Dutkiewicz, M.; Scaria, V.; Hariharan, M.; Maiti, S.; Kurreck, J. Inhibition of translation in living eukaryotic cells by an RNA G-quadruplex motif. *RNA* **2008**, *14*, 1290−1296.

(28) Shahid, R.; Bugaut, A.; Balasubramanian, S. The BCL-2 5′ untranslated region contains an RNA G-quadruplex-forming motif that modulates protein expression. *Biochemistry* **2010**, *49*, 8300−8306.

(29) Bugaut, A.; Balasubramanian, S. 5′-UTR RNA G-quadruplexes: translation regulation and targeting. *Nucleic Acids Res.* **2012**, *40*, 4727−4741.

(30) Morris, M. J.; Negishi, Y.; Pazsint, C.; Schonhoft, J. D.; Basu, S. An RNA G-quadruplex is essential for cap-independent translation initiation in human VEGF IRES. *J. Am. Chem. Soc.* **2010**, *132*, 17831−17839.

(31) Thomas, J. R.; Hergenrother, P. J. Targeting RNA with small molecules. *Chem. Rev.* **2008**, *108*, 1171−1224.

(32) Rouleau, S. G.; Beaudoin, J. D.; Bisaillon, M.; Perreault, J. P. Small antisense oligonucleotides against G-quadruplexes: specific mRNA translational switches. *Nucleic Acids Res.* **2015**, *43*, 595−606.

(33) Bugaut, A.; Rodriguez, R.; Kumari, S.; Hsu, S. T.; Balasubramanian, S. Small molecule-mediated inhibition of translation by targeting a native RNA G-quadruplex. *Org. Biomol. Chem.* **2010**, *8*, 2771−2776.

(34) Halder, K.; Largy, E.; Benzler, M.; Teulade-Fichou, M. P.; Hartig, J. S. Efficient suppression of gene expression by targeting 5′-UTR-based RNA quadruplexes with bisquinolinium compounds. *ChemBioChem* **2011**, *12*, 1663−1668.

(35) Ito, K.; Go, S.; Komiyama, M.; Xu, Y. Inhibition of translation by small RNA-stabilized mRNA structures in human cells. *J. Am. Chem. Soc.* **2011**, *133*, 19153−19159.

DOI: 10.1021/acs.jmedchem.5b00139
J. Med. Chem. XXXX, XXX, XXX−XXX

(36) Satyanarayana, M.; Kim, Y. A.; Rzuczek, S. G.; Pilch, D. S.; Liu, A. A.; Liu, L. F.; Rice, J. E.; LaVoie, E. J. Macrocyclic hexaoxazoles: Influence of aminoalkyl substituents on RNA and DNA G-quadruplex stabilization and cytotoxicity. *Bioorg. Med. Chem. Lett.* **2010**, *20*, 3150−3154.
(37) Su, Z.; Zhang, Y.; Gendron, T. F.; Bauer, P. O.; Chew, J.; Yang, W. Y.; Fostvedt, E.; Jansen-West, K.; Belzil, V. V.; Desaro, P.; Johnston, A.; Overstreet, K.; Oh, S. Y.; Todd, P. K.; Berry, J. D.; Cudkowicz, M. E.; Boeve, B. F.; Dickson, D.; Floeter, M. K.; Traynor, B. J.; Morelli, C.; Ratti, A.; Silani, V.; Rademakers, R.; Brown, R. H.; Rothstein, J. D.; Boylan, K. B.; Petrucelli, L.; Disney, M. D. Discovery of a Biomarker and Lead Small Molecules to Target r(GGGGCC)-Associated Defects in c9FTD/ALS. *Neuron* **2014**, *83*, 1043−1050.
(38) Ofer, N.; Weisman-Shomer, P.; Shklover, J.; Fry, M. The quadruplex r(CGG)n destabilizing cationic porphyrin TMPyP4 cooperates with hnRNPs to increase the translation efficiency of fragile X premutation mRNA. *Nucleic Acids Res.* **2009**, *37*, 2712−2722.
(39) Liu, Z. Q.; Zhuo, S. T.; Tan, J. H.; Ou, T. M.; Li, D.; Gu, L. Q.; Huang, Z. S. Facile syntheses of disubstituted bis(vinylquinolinium)-benzene derivatives as G-quadruplex DNA binders. *Tetrahedron* **2013**, *69*, 4922−4932.
(40) Faudale, M.; Cogoi, S.; Xodo, L. E. Photoactivated cationic alkyl-substituted porphyrin binding to g4-RNA in the 5′-UTR of KRAS oncogene represses translation. *Chem. Commun. (Cambridge, U. K.)* **2012**, *48*, 874−876.
(41) Morris, M. J.; Wingate, K. L.; Silwal, J.; Leeper, T. C.; Basu, S. The porphyrin TmPyP4 unfolds the extremely stable G-quadruplex in MT3-MMP mRNA and alleviates its repressive effect to enhance translation in eukaryotic cells. *Nucleic Acids Res.* **2012**, *40*, 4137−4145.
(42) Sissi, C.; Gatto, B.; Palumbo, M. The evolving world of protein-G-quadruplex recognition: a medicinal chemist's perspective. *Biochimie* **2011**, *93*, 1219−1230.
(43) von Hacht, A.; Seifert, O.; Menger, M.; Schutze, T.; Arora, A.; Konthur, Z.; Neubauer, P.; Wagner, A.; Weise, C.; Kurreck, J. Identification and characterization of RNA guanine-quadruplex binding proteins. *Nucleic Acids Res.* **2014**, *42*, 6630−6644.
(44) Wolfe, A. L.; Singh, K.; Zhong, Y.; Drewe, P.; Rajasekhar, V. K.; Sanghvi, V. R.; Mavrakis, K. J.; Jiang, M.; Roderick, J. E.; Van der Meulen, J.; Schatz, J. H.; Rodrigo, C. M.; Zhao, C.; Rondou, P.; de Stanchina, E.; Teruya-Feldstein, J.; Kelliher, M. A.; Speleman, F.; Porco, J. A., Jr.; Pelletier, J.; Ratsch, G.; Wendel, H. G. RNA G-quadruplexes cause elF4A-dependent oncogene translation in cancer. *Nature* **2014**, *513*, 65−70.
(45) Bidzinska, J.; Cimino-Reale, G.; Zaffaroni, N.; Folini, M. G-quadruplex structures in the human genome as novel therapeutic targets. *Molecules* **2013**, *18*, 12368−12395.
(46) Brooks, T. A.; Hurley, L. H. Targeting MYC expression through G-quadruplexes. *Genes Cancer* **2010**, *1*, 641−649.
(47) Zamiri, B.; Reddy, K.; Macgregor, R. B., Jr.; Pearson, C. E. TMPyP4 porphyrin distorts RNA G-quadruplex structures of the disease-associated r(GGGGCC)n repeat of the C9orf72 gene and blocks interaction of RNA-binding proteins. *J. Biol. Chem.* **2013**, *289*, 4653−4659.
(48) Lee, Y. B.; Chen, H. J.; Peres, J. N.; Gomez-Deza, J.; Attig, J.; Stalekar, M.; Troakes, C.; Nishimura, A. L.; Scotter, E. L.; Vance, C.; Adachi, Y.; Sardone, V.; Miller, J. W.; Smith, B. N.; Gallo, J. M.; Ule, J.; Hirth, F.; Rogelj, B.; Houart, C.; Shaw, C. E. Hexanucleotide repeats in ALS/FTD form length-dependent RNA foci, sequester RNA binding proteins, and are neurotoxic. *Cell Rep.* **2013**, *5*, 1178−1186.
(49) Mori, K.; Lammich, S.; Mackenzie, I. R.; Forne, I.; Zilow, S.; Kretzschmar, H.; Edbauer, D.; Janssens, J.; Kleinberger, G.; Cruts, M.; Herms, J.; Neumann, M.; Van Broeckhoven, C.; Arzberger, T.; Haass, C. hnRNP A3 binds to GGGGCC repeats and is a constituent of p62-positive/TDP43-negative inclusions in the hippocampus of patients with C9orf72 mutations. *Acta Neuropathol.* **2013**, *125*, 413−423.

DOI: 10.1021/acs.jmedchem.5b00139
J. Med. Chem. XXXX, XXX, XXX−XXX